Available online at www.sciencedirect.com
ScienceDirect
Catalysis Today 120 (2007) 2–20
CATALYSIS TODAY
www.elsevier.com/locate/cattod

Selective oxidations in micro-structured catalytic reactors—For gas-phase reactions and specifically for fuel processing for fuel cells

G. Kolb [a,*], V. Hessel [a,b,**], V. Cominos [a], C. Hofmann [a], H. Löwe [a], G. Nikolaidis [a], R. Zapf [a], A. Ziogas [a], E.R. Delsman [b], M.H.J.M. de Croon [b], J.C. Schouten [b,**], O. de la Iglesia [c], R. Mallada [c], J. Santamaria [c,**]

[a] *Institut für Mikrotechnik Mainz GmbH, Carl-Zeiss-Str. 18-20, 55129 Mainz, Germany*
[b] *Eindhoven University of Technology, P.O. Box 513, 5600 MB Eindhoven, the Netherlands*
[c] *University of Zaragoza, 50009 Zaragoza, Spain*

Available online 28 August 2006

Abstract

This review on selective oxidations is split into two parts. The first part concerns catalytic gas-phase oxidation reactions in micro-reactors, typically being performed in wall-coated micro-channels [V. Hessel, G. Kolb, J.C. Schouten, V. Cominos, C. Hofmann, H. Löwe, G. Nikolaidis, R. Zapf, A. Ziogas, E.R. Delsman, M.H.J.M. de Croon, O. de la Iglesia, R. Mallada, J. Santamaria, in: S. Ernst, E. Gallei, J.A. Lercher, Rossini, E. Santacesaria (Eds.), Conference pre-prints of the DGMK/SCI-Conference ''Oxidation and Functionalization: Classical and Alternative Routes and Sources'', Milan, Italy, October 12–14, 2005 [1] (see also acknowledgements at the end of the article)]. Liquid and gas–liquid oxidations are not included due to their different reactor design and way of processing. This comprises process development for fine chemical intermediates or bulk chemicals. By example of different reactions, the benefits of micro-chemical process engineering are shown. While there are numerous engineering reasons, one major driver is the increase of selectivity by diminishing side and follow-up reactions, most often the total oxidation to carbon dioxide, through preventing or at least decreasing hot spot formation. Another major advantage of micro-reactors is that mass-transfer resistances can be suppressed, thereby giving access to intrinsic kinetics. In the second part, we describe selective oxidation as one gas purification step in the framework of fuel processing for fuel cells, which is most often termed preferential oxidation in this context. Here, the selectivity towards carbon monoxide formation by diminishing the hydrogen oxidation is a major driver. The current developments are grouped so that all facets from kinetic modelling, heat transfer studies, catalyst testing, reactor and integrated-system engineering up to process engineering, exergy analysis, performance benchmarking and operation under real-case process flows are covered.

Keywords: Catalytic reactor; Micro-channels; Oxidation

1. Selective oxidations for fine chemical intermediates and bulk chemicals

Catalytic micro-channel reactors have unique flow and heat and mass transfer properties, which have led in the last years to process improvements for a number of gas-phase processes, among them selective hydrogenations and oxidations [2–5]. Selective oxidation refers to elemental reactions that stop either at a partly oxidised, intermediate species of value, while the formation of the totally oxidised, final product is not desired, e.g. carbon dioxide. Next to this consecutive reaction scenario, there can be also competitive, parallel oxidation reactions within a gas mixture, from which only one route is favoured. An example is preferential oxidation (PrOx) as a gas purification step.

In the case of consecutive reactions, accurate setting of the gas residence time and avoidance of hot spots are the major incentives for applying micro-channel reactors to enhance selectivity. In addition, the superb mass transfer properties of micro-channel reactors offer a useful tool to optimally control gas concentration profiles in the reactor to suppress an

* Corresponding author. Tel.: +49 6131 990 341; fax: +49 6131 990 305.
** Corresponding authors.
E-mail address: kolb@imm-mainz.de (G. Kolb).

0920-5861/$ – see front matter © 2006 Elsevier B.V. All rights reserved.
doi:10.1016/j.cattod.2006.07.021

influence of mass transfer on the overall kinetics as well as gas adsorption and desorption at the catalyst surface. These advantages of micro-reactor technology also apply to preferential oxidation, for example, in the case of two parallel oxidation routes, one involving hydrogen and the other carbon monoxide. Here, the availability of new catalysts with high selectivity for carbon monoxide oxidation is of central importance.

1.1. Oxidation of ammonia to dinitrogen or nitrogen oxide

Ammonia (NH_3) oxidation products are dinitrogen oxide (N_2O), nitrogen oxide (NO) and nitrogen (N_2), depending on the process conditions [6–8]. N_2O is a well-known selective oxidising agent, for example, for phenol synthesis from benzene over a zeolite catalyst. In a modular micro-reactor design with integration of reaction channels and outlet coolers, NO formation was decreased in favour of N_2O, even at a large surplus of oxygen [6]. In another reactor-design oriented study, monolith, parallel multi-plate and micro-channel reactors were benchmarked for their NH_3 conversion performance (see Fig. 1) [7]. Besides different reactor concepts, the various symbols stand for different catalyst loadings, since the reactor type was coupled to a specific way of catalyst deposition and this correlates with the maximum amount of achievable catalyst loading. It was found that the achievable maximum catalyst loading was decisive for the reaction behaviour, whereas the type of reactor seems to have no influence here, i.e. all reactors were operated under similar mass and thermal conditions and have similar hydraulic diameters, although the reactor geometries were made by different fabrication and assembly techniques.

Another example of the benefits of micro-reactor operation is demonstrated by the integration of ultra-thin minaturized

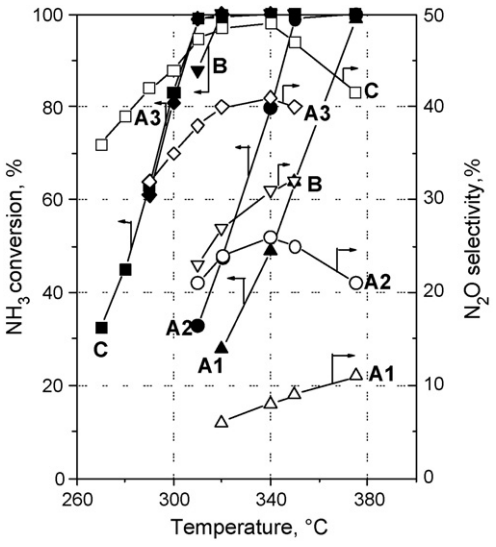

Fig. 1. Conversion of NH_3 (open symbols) and selectivity to N_2O (closed symbols) for the ammonia-oxidation process on Pt catalyst. Micro-reactors A1 (▲), A2 (●), A3 (◆), B (▼) and C (■) were used [6]. A1–A3 are parallel multi-plate reactors of different catalyst loadings, B is a monolith reactor and C a micro-channel reactor (for more details see ref. [6]).

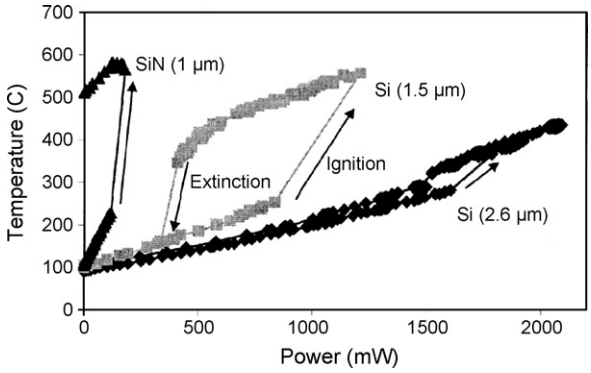

Fig. 2. Change of hysteresis loop for the ammonia oxidation in a micro-reactor, when varying the material and thickness of a thin free-standing layer acting as catalytic material and to remove reaction heat ('membrane'). Heat conductance and heat transfer resistance change thereby.

heaters within a reactor, accomplished by MEMS-type micro-machining and assembly (micro-electro-mechanical systems, MEMS) [9–12]. Direct coupling of heating and reaction is achieved when the micro-heater is made out of catalytic material, e.g. by using thin platinum foil as a free standing membrane. In that case, fast temperature changes can be realised at the catalytic site with simultaneous fast removal of the reaction heat by keeping the heat transfer resistance low (small membrane thickness) and the heat conductance high (appropriate choice of membrane material). In this way, the well-known ignition-extinction behaviour and related conversion-temperature hysteresis as present in conventional reactors can be avoided (see Fig. 2).

This offers flexibility in selecting the appropriate process regime for achieving a required product selectivity. Especially, in the non-hysteresis zones the benefits of the micro-structure thermal management are fully exploited, by utilizing novel, otherwise unreachable ('hidden') process regimes, which can give a unique product distribution. Similar selectivity effects for industrially valuable reactions, such as selective oxidations of double bonds, yielding epoxides, or oxidations to anhydrides, ketones and alcohols, still wait for verification.

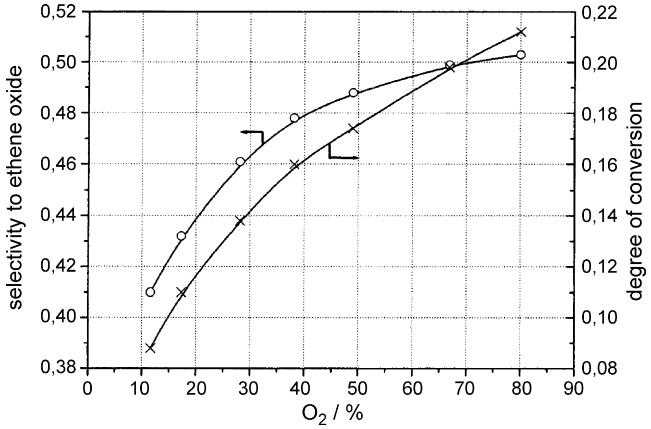

Fig. 3. Experimental results for the selectivity and the degree of conversion of ethylene as a function of oxygen concentration [13].

Table 1
Process parameters for an industrial ethylene oxide process compared to parameters achieved for micro-reactors machined by different techniques [15]

	Oxygen-based industrial process	Micro-reactor-based process, laser-LIGA -micro-channels	Micro-reactor-based process, etched micro-channels	Micro-reactor-based process, Aluchrom micro-channels
C_2H_4 (vol.%)	15–40	1.5–6	3–15	15
O_2 (vol.%)	5–9	10–41	5–85	85
CH_4 (vol.%)	1–60			
Temperature (°C)	220–275	240–290	240–290	270
Pressure (bar)	10–22	5	2–20	5
Residence time (s)	0.9–1.8	0.1–0.2	0.1–1.5	1.2
C_2H_4 conversion (%)	7–15	2–15	5–20	2–6
Selectivity (%)	80	44–69	38–69	42–58
Space–time yield (t/(h m^3)	0.13–0.26 (reactor)	0.01–0.07 (foils), 0.14–0.78 (channels)	0.03–0.13 (foils) 0.18–0.67 (channels)	0.01–0.06 (foils), 0.08–0.36 (channels)

1.2. Oxidation of ethylene to ethylene oxide

Ethylene oxide synthesis is of large industrial importance and is performed in world-scale plants in the 100,000 t/a range.

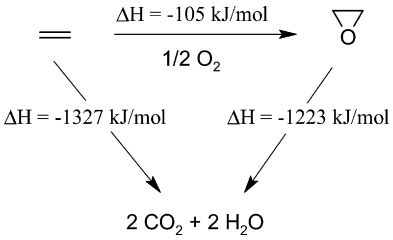

Safety is an important issue as the enthalpy of the total oxidation reaction is more than ten times larger than that of the ethylene oxide formation. Hot spots in the reactor can be present as a result of large heat releases during total oxidation, which decrease selectivity and may lead to a runaway of the reaction. To prevent this, typical measures are adding methane as inert gas, restricting to low oxygen-to-ethylene ratios and use of promoters, which enhance selectivity but decrease productivity (space–time yield). Studies in micro-channel reactors showed safe operation in the explosive regime at reactant concentrations of 20 vol.% ethylene and 80% oxygen (no inert gas) at a pressure of 3 bar (see Fig. 3) [13].

Conversions up to 20% were reported, being higher than for fixed-bed operation with the same catalyst and approaching or slightly exceeding best industrial catalysts' conversion [14,15]. This implies that the space–time yield of the micro-reactor operation is within reach of industrial reactors, at least when ignoring the channel-encasing reactor material volume (Table 1). However, the best micro-channel coated catalyst selectivities did so far not exceed 70% and are thus still far from the industrial target of 80% [14,15]. It stands to reason that even higher selectivities of 85–90% will be needed to gain industry's interest by step-changing the cost estimations. However, so far micro-reactor operation is simpler than industrial practice, i.e. no promoters are added.

1.3. Oxidation of 1-butene to maleic anhydride

The oxidation of 1-butene to maleic anhydride is another example of a selective oxidation reaction in combination with the strongly exothermic total oxidation to carbon dioxide.

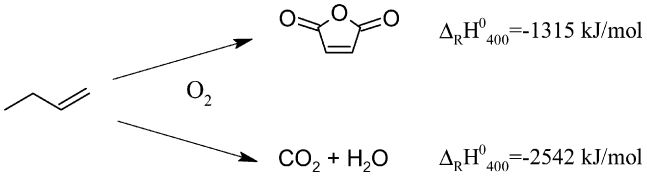

The selective oxidation of the C4-hydrocarbon is a highly exothermic process as well ($\Delta H^{\circ}_{R,400} = -1315\,kJ/mol$). In addition, the selectivity to maleic anhydride is low, being determined by multiple reaction pathways where furan is one major intermediate. The catalyst employed in a micro-channel reactor was $V_2O_5/P_2O_5/TiO_2$ [16]. Selectivities higher than 32% were achieved for micro-reactor operation at conversions up to 90%, which is similar to fixed-bed performance. Safe operation in micro-reactors was achieved at 1-butene concentrations (5–15%; 0.1 MPa; 400 °C), which were up to 10 times higher than the explosion limit. The space–time yields of

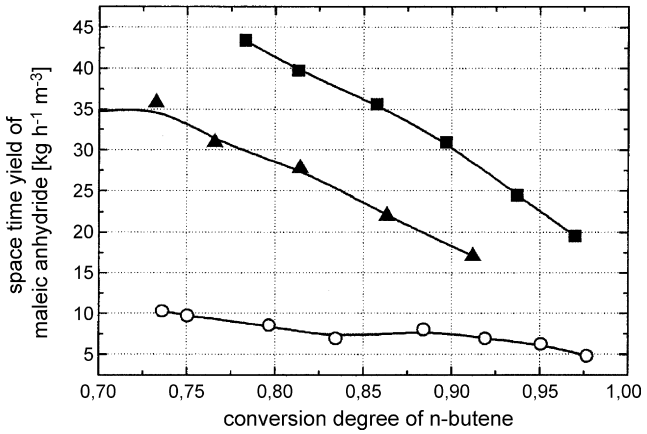

Fig. 4. Space–time yield of maleic anhydride vs. degree of conversion for n-butene when using different reactor types. (■) 0.08-mm micro-channel reactor and (▲) 0.2-mm micro-channel reactor; (○) fixed-bed reactor [16].

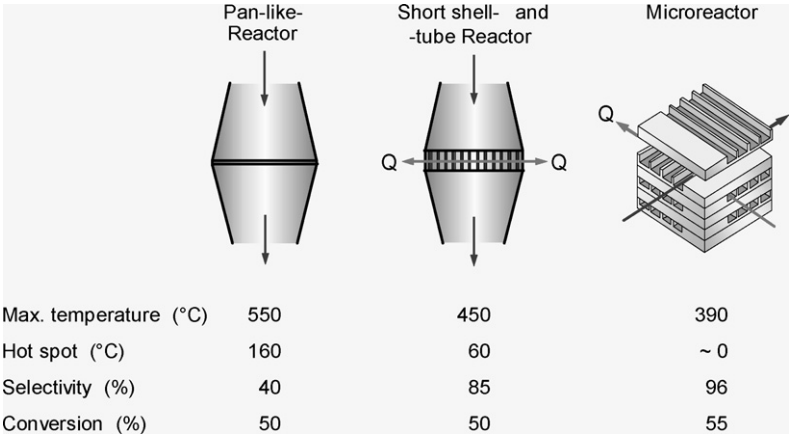

Max. temperature (°C)	550	450	390
Hot spot (°C)	160	60	~ 0
Selectivity (%)	40	85	96
Conversion (%)	50	50	55

Fig. 5. Performance data of a micro-reactor benchmarked to two industrially used reactor concepts, pan-like and short shell-and-tube reactors for the selective oxidation of a labile alcohol to the respective aldehyde [17].

the micro-channel reactor (based on the whole plate volume, i.e. including wall material) were five times larger than those of a conventional fixed-bed reactor (see Fig. 4) due to the shorter residence time in the micro-reactor.

1.4. Oxidation of alcohol with labile group to aldehyde

Process development studies on selective aldehyde formation from undisclosed gaseous alcohols with a second thermally labile moiety over silver catalyst were conducted by BASF using a micro-channel reactor [17].

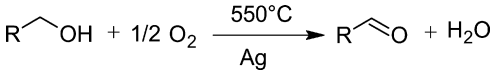

A comparison was made of the selectivity-conversion performance in the micro-channel reactor and in industrial-type pilot and production-scale reactors, such as pan-like and (long and short-sized) multi-tube reactors. The industrial reactors were not able to meet the selectivity targets, since the key to achieving selectivity was having both short residence times and avoidance of hot spots and only one of these requirements could be met. The micro-structured reactor could be operated at the desired flow and heat management conditions, resulting in a selectivity of 96% at 55% conversion (pan-like reactor: 40%/50%; short shell-and-tube reactor-heat exchanger: 85%/50%; Fig. 5). In addition, the reaction temperature could be lowered from 550 to 390 °C in the micro-reactor due to better heat and mass transfer, which also reduced thermally induced side and follow-up reactions.

1.5. Oxidation of 3-methyl-2-buten-1-ol to 3-methyl-2-buten-1-al

Silicon–glass micro-fabricated reactors containing silver catalyst were used for oxidative dehydrogenation of 3-methyl-2-buten-1-ol to the corresponding aldehyde [18].

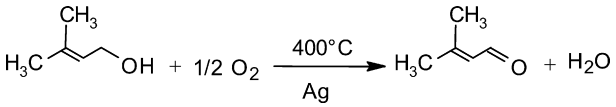

The reactors were safely operated in a wide range of oxygen concentrations, in a temperature range of 310–464 °C and residence times of 15–50 ms. High selectivities were obtained at high alcohol and low oxygen concentrations. Conversion of 60–70% with high selectivity (~95%) at alcohol concentrations of 4–7.2 vol.% was achieved at an oxygen/alcohol ratio of ~1 and reaction temperature of 400 °C. The conversion increased with temperature without ignition. The selectivity decreased above 415 °C due to formation of carbon monoxide, carbon dioxide and higher molecular weight by-products (see Fig. 6).

1.6. Oxidation of isoprene to citraconic anhydride

The oxidation of isoprene to citraconic anhydride using $V_{30}Ti_{70}O_x$ catalyst or $V_{30}Ti_{70}O_x$–SiO_2 catalyst indicated the influence of the reactor material blank activity on selectivity [19].

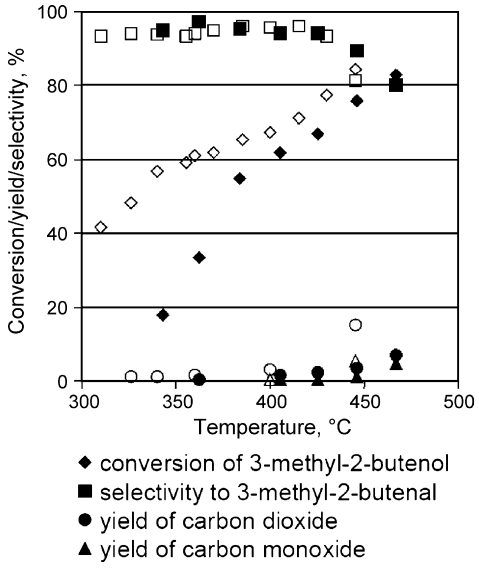

Fig. 6. Effect of reaction temperature on alcohol conversion, aldehyde selectivity and yield of CO and CO_2 (Solid symbols: micro-reactor with 220 μm channel depth; hollow symbols: micro-reactor with 60 μm channel depth; 3-methyl-2-butenol = 4 vol.%, O_2: 4.5 vol.%, He as balance.) [18].

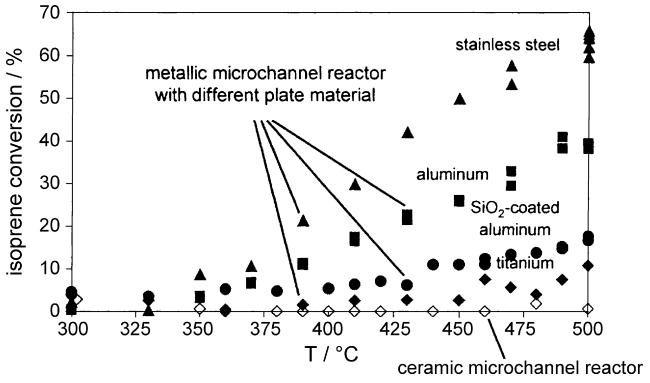

Fig. 7. Experimental results for isoprene conversion in a ceramic micro-reactor in absence of catalyst (◇). Experimental values for different reactor materials (full symbols) [19].

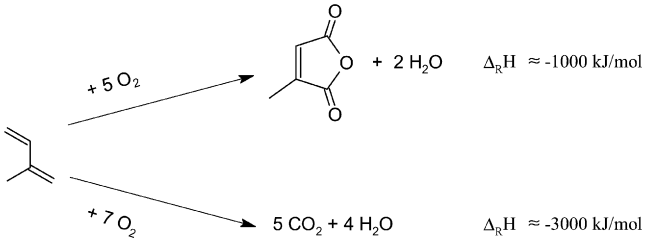

Micro-structured reactors have relatively large surface areas per unit volume and thus the effect of the reactor channel-wall material on conversion and selectivity can be expected to be much more significant than in conventional reactors. Indeed, 60% unselective conversion was observed for the citraconic anhydride process in absence of a catalyst (blank test) when employing a steel micro-reactor (see Fig. 7).

This could be reduced with a ceramic reactor material to 1–2%. The maximum citraconic acid selectivity was 25% at full conversion for suspension catalysts, while a lower selectivity was obtained using a catalyst based on anodic oxidation and impregnation.

1.7. HCN formation via Andrussov process

A similar effect of the reactor material on conversion was observed in case of HCN formation in a micro-reactor (Andrussov process) [20].

$$CH_4 + NH_3 + \tfrac{3}{2}O_2 \rightarrow HCN + 3H_2O \quad \Delta H = -474\,\mathrm{kJ/mol}$$

In this study, total oxidation to carbon dioxide and soot deposition downstream of a micro-structured catalyst hole array were found, the latter being indicative of unselective oxidation. The HCN yield of 31% was about half of that of the industrial process, but at relatively high ammonia selectivity of 62%. Micro-reactor tests were conducted both at BASF and Rhodia, giving different results due to different processing conditions (see Fig. 8). In addition, the micro-reactor performance was compared to monoliths (results not shown here). It was better than that of coiled-strip metal monoliths and straight-channel ceramic monoliths run under laminar flow conditions, and was nearly similar to irregular-pore ceramic monoliths operated at turbulent flow conditions. The micro-structured reactor showed local temperatures up to 1000 °C as well as high mass transfer rates (high conversion) even at millisecond contact time with flow-through passages of less than 250 μm.

1.8. Oxi-hydrogen reaction to hydrogen peroxide

Reaction of hydrogen and oxygen to form hydrogen peroxide in the explosive regime was also conducted in micro-channel reactors.

$$2H_2 + O_2 \rightarrow 2H_2O \quad \Delta H = -241\,\mathrm{kJ/mol}$$

unselective oxidation to water

$$H_2 + O_2 \rightarrow H_2O_2$$

selective oxidation to hydrogen peroxide

Safe operation without explosion was demonstrated at temperatures up to 1200 °C (in this case making water only) [21,22]. Widening of the safe operation envelope could be achieved by using the flame-arrestor effect of micro-channels [21]. This is a result of the chain reaction extinction mechanism at the channel walls rather than just enhanced heat transfer. In this way, the explosion regimes shift by reactor volume miniaturization so that former hazardous regimes can be safely explored (see Fig. 9). The micro-reactor envelope depends on the thermal boundary conditions, i.e. the assumption of the micro-channel wall temperature (see Fig. 9).

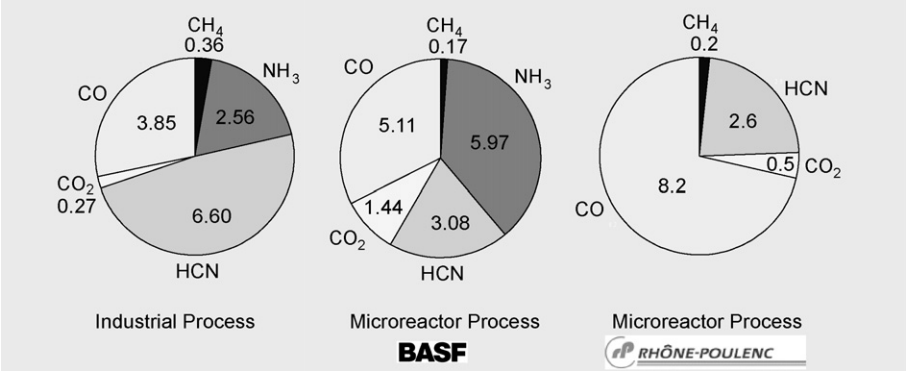

Fig. 8. Product distributions obtained by measurements of BASF and Rhône-Poulenc compared to results of an industrial process (vol.% of the reactant mixture; the remainder being oxygen and nitrogen) [20].

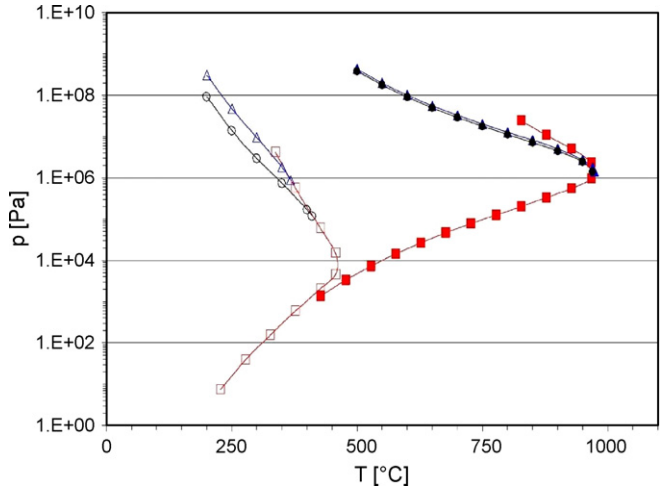

Fig. 9. Extending kinetic explosion (squares) and thermal explosion limits by using a micro-reactor with 300 μm channel diameter (filled symbols). Calculated values for $T_{wall} = T_{room}$ (○) and $T_{wall} = T_{reaction}$ (△); T_{wall}, T_{room} and $T_{reaction}$ being the temperatures of the micro-channel wall, room temperature and reaction temperature. Comparison with 1 m diameter (open symbols) [21].

Hydrogen peroxide was also produced in a trickle-bed reactor with a gas–liquid flow and a particulate catalyst [23]. Selectivities up to 75% were reported at nearly full conversion (Table 2). Full conversion is relevant for avoiding the need for safe downstream operation in micro-structured processing units functioning as flame-arrestors. Currently, there are three industrial projects known aiming at commercial implementation of this direct production route.

2. Preferential oxidation (PrOx) for fuel processing

2.1. Fuel reforming

Fuel reforming is an alternative method for providing H_2 on demand to proton exchange membrane (PEM) fuel cells but requires CO clean-up stages, such as water–gas shift reactors (with exception of methanol reforming systems) followed by either pressure swing adsorption, methanation or selective oxidation as even trace amounts of CO can poison the fuel cell catalyst. CO removal by pressure swing adsorption requires expensive compressors, which cannot be applied easily in small scale systems. Methanation is a less advanced technology and becomes more complex due to the hydrogenation of CO_2 present in the reformate. Since CO selective oxidation takes place at low temperatures and atmospheric pressure, and is relatively inexpensive, it is considered to be a practical method with high potential. CO levels need to be decreased to values below 10 ppm as dictated by the poisoning limit of a conventional low-temperature PEM fuel cell Pt catalyst [24]. This value may be increased to 50 ppm or higher in case Pt-Ru catalysts are applied. CO levels in the off-gas of a water–gas shift reactor typically lie between 0.5 and 2 vol.% and not significantly more than 1 vol.% is contained in the off-gas of a methanol reformer. In the literature, only a few papers report the decrease of CO concentrations down to ppm levels [25,26–28]. Micro-reactors show large promise in the development of miniature fuel processors for small scale electricity production, where several unit operations can be integrated with micro-structured sensors and actuators to form a micro hydrogen producing plant [29].

Table 2
Specs of the direct hydrogen-peroxide micro-reactor process benchmarked [23]

	Published	IMM-UOP test
Pressure (bar)	124	30
Temperatur (°C)	35	50
O_2:H_2	6.8	3
Space velocity (g H_2/(g_{CAT} h))	2.6	1.8
H_2O_2 concentration (max) (wt.%)	5.2	1.7[a]
Yield (g H_2O_2/(g_{CAT} h))	1.5	2.0

[a] Not optimized.

2.2. Prefential oxidation (PrOx)

The removal of small traces of carbon monoxide in pre-cleaned reformate flows in hydrocarbon reformers is commonly performed by the oxidation with air. In the case of methanol reforming, the reformate gas is directly sent to a preferential oxidation unit as the carbon monoxide concentration is already sufficiently low as a result of the low-temperature methanol reforming:

$$CO + 0.5O_2 \rightarrow CO_2 \quad \Delta H_R = -283\,kJ/mol$$

Part of the hydrogen present will be oxidised as well in an undesired side reaction:

$$H_2 + 0.5O_2 \rightarrow H_2O \quad \Delta H_R = -242\,kJ/mol$$

In an oxygen deficient atmosphere in a PrOx reactor, carbon monoxide can be formed again by the reverse water–gas shift reaction (r-WGS):

$$H_2 + CO_2 \rightarrow H_2O + CO \quad \Delta H_R = +41\,kJ/mol$$

2.3. Methodological approaches for PrOx catalyst testing and optimisation

A methodological based study aimed at combining the advantages of a knowledge-based selective combinatorial approach with the fundamental characterization and single reactor kinetic studies for the preferential oxidation [30]. Using the former, an effective tool to accelerate the discovery of new catalytic materials is provided, while the latter is needed for the most active samples to iterate to further optimize the activity and selectivity of the catalysts. By in situ infrared thermography (IRT), a large data set on coarse catalytic activity is achieved simultaneously for an array of various samples under model reaction conditions. Then, a 10-channel parallel-flow reactor (COMBI Reactor™ [31]) is used to measure sequentially the activity of 10 of the most active samples. Each COMBI-Reactor system includes a flow control system,

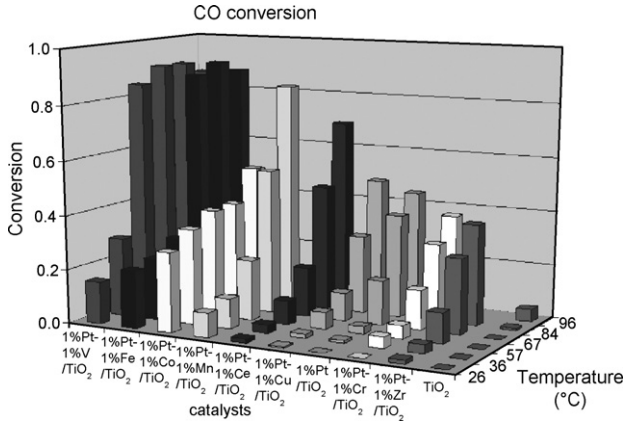

Fig. 10. Conversion and selectivity for a second generation family of catalysts obtained on the COMBI Reactor™. All active components supported on TiO_2. Reactant composition: $CO:O_2:H_2 = 1:2:40$, balance helium. Total flow: each well 60 cm^3/min [30].

the reactor module, an oven, a series of switching valves and a micro-GC. The reactor module has two inlets, a mixing chamber and 10 wells to load 10 different samples. The entire module fits into an oven for isothermal operation. The switching valves supply sequential samples to the micro-GC for analysis that gives quick, realistic results.

In this way, activity trends for the PrOx reaction at low temperature were given, showing that platinum on TiO_2 carrier is more active than being on Al_2O_3 carrier (see Fig. 10, for an optimised family of catalysts) [30]. The promotion of Pt/TiO_2 catalysts with ceria provides sites that enhance CO conversion and selectivity at low temperature. The highest activity and selectivity was exhibited by a 1% Pt-15% CeO_2/TiO_2 catalyst below 100 °C, whereas the unpromoted Pt/Al_2O_3 appears to be the best catalyst at 100 °C and higher temperatures. The catalyst pre-treatment in multi-tube reactors is the key to getting the proper reduction and high metal dispersion.

2.4. Transport resistance studies—systemic comparison of micro-reactors to minimized packed-bed reactors (m-PBRs)

A kinetic study on preferential oxidation was concerned with benchmarking the micro-reactor performance to that of conventional lab-scale equipment, minimized packed-bed reactors (m-PBRs) [32]. For this purpose, internal and external transfer limitations were analyzed and a mechanistic model for the elemental steps in reaction and heat transfer was proposed.

First, it was demonstrated that wall-coated dense Pt/Al_2O_3 thin-film catalysts in silicon micro-reactors exhibited similar PrOx activity as other literature catalyst systems based on similar formulation, which is a fundamental for comparison of the two reactor approaches [32]. Superior heat transport properties were found with the micro-reactor compared to those of conventional lab reactors (m-PBRs) according to the comparison of the Damköhler numbers (*Da*) for both systems. The minimized heat-transport resistance of the thin-film catalyst efficiently suppresses the reverse water–gas shift (r-WGS) reaction, which would severely compromise the

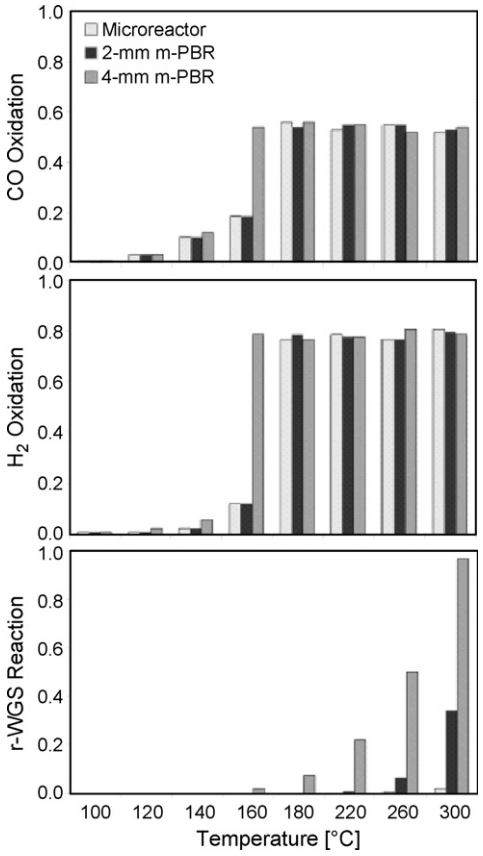

Fig. 11. The average reaction rates for CO oxidation, H_2 oxidation and the r-WGS reaction at T_w = 120, 180, 220 °C for the micro-reactor, 2- and 4-mm m-PBR's. All vertical axes have the same scales, with full scale (1.0) corresponding to 3.9 mol/(kg s) [32].

overall PrOx performance, thereby greatly enlarging the operating temperature window (see Fig. 11). At low temperatures (<220 °C), negligible mass- and heat-transport resistance is given, so that the experiments directly reveal intrinsic kinetics. Above 220 °C, however, external mass transport limits the overall reaction rates for PrOx.

In another study, similar conclusions on transport resistances were drawn [33]. It was found that no external mass transfer limitations are given, different from the packed-bed micro-reactor. Limitations may arise only by internal diffusion within the porous catalyst itself. This is a material (and no reactor engineering) problem and can be overcome by achieving suited pore micro-structures, which would be the same for the micro and packed bed reactor.

2.5. Heat-transfer studies—systemic comparison of micro-reactors to minimized packed-bed reactors (m-PBRs)

A separate reactor model using the finite-difference method was applied to give more detailed insight in the above mentioned systemic differences in performance of the micro-reactor and m-PBRs for the temperature dependency of the CO conversion [34]. A quasi-3D tubular non-isothermal reactor model based on the finite difference method was used to quantitatively study the effect of heat transport resistance on

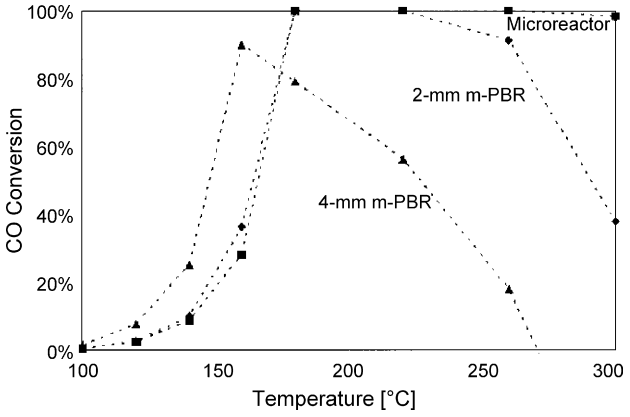

Fig. 12. Calculated CO conversion vs. different reactor wall temperatures for the micro-reactor, 2- and 4-mm m-PBRs. WHSV: 1500 h^{-1} [34].

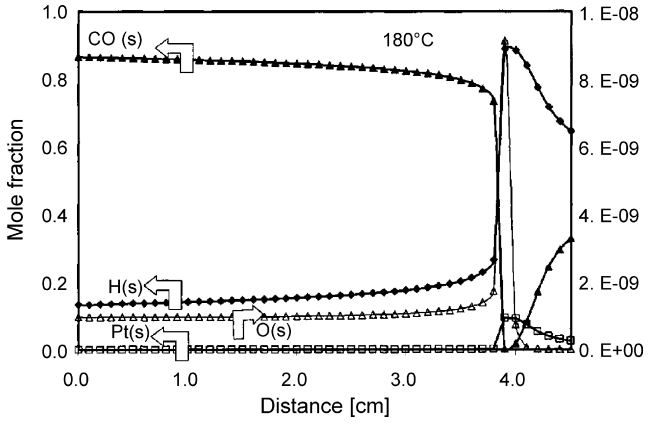

Fig. 13. CHEMKIN simulation for the mole fractions of surface species as a function of residence time (here expressed as channel length) [35].

PrOx reaction behavior. Kinetic expressions for the three principal reactions involved were formed and their parameters were evaluated with a non-linear regression method. Based on the resulting kinetic model and an energy balance derived for PrOx, the finite difference method was then adopted for the quasi-3D model.

The temperature gradients in m-PBRs speed up the reverse water–gas shift (r-WGS) reaction, thereby considerably narrowing the range of possible operating temperatures [34]. In turn, the high heat removal of the thin-film catalyst on the micro-channel allows for isothermal operations without temperature gradients and in this way prevents the onset of the r-WGS reaction. For wall temperatures before and during light-off, small local temperature gradients in the m-PBR's cause the light-off curve to shift to lower temperatures. At somewhat higher temperatures, large temperature gradients rapidly develop in the m-PBR's. This degrades the PrOx performance by activating the r-WGS reaction and decreasing the net CO conversion (see Fig. 12).

2.6. Kinetic studies—simulation of elemental steps

Numerical simulations of the reaction system were performed applying CHEMKIN software and a network of 8 species in the gas phase, 8 surface species and 28 reactions. The simulation described the experimental performance of the reactor very well. It revealed that CO oxidation occurs by the reaction between adsorbed CO and OH species and not by the reaction between adsorbed CO and O species, as the rate of the latter reaction was 10 orders of magnitude lower. A simplified reaction mechanism could be formulated (S: Surface) [35].

$$O_2 + 2Pt(S) \rightarrow 2O(S)$$

$$H_2 + 2Pt(S) \rightarrow 2H(S)$$

$$O(S) + H(S) \rightarrow OH(S)$$

$$CO(S) + OH(S) \rightarrow CO_2(S) + H(S)$$

$$CO_2(S) \rightarrow CO_2$$

The simulation revealed that the catalyst surface was almost completely covered by carbon monoxide up to certain channel length (gas residence time), and then abruptly decreased, when no carbon monoxide was left in the gas phase (see Fig. 13) [35]. At the same time, the concentrations of adsorbed oxygen and hydrogen increased by almost an order of magnitude, which lead to a consumption of hydrogen due to water formation. The degree of water formation was merely limited by the amount of oxygen present in the gas phase. When all carbon monoxide and water were consumed, carbon monoxide was formed again via the reverse water–gas shift reaction.

In a follow-up study, a micro-kinetic reaction model for PrOx was used to investigate further reaction pathways and surface intermediate species and to conclude on the impact of temperature uniformity on the CO oxidation selectivity [34]. Before CO light-off, the Pt surface is covered by adsorbed CO. The adsorption of O_2 is rate limiting at low temperatures. At higher temperatures, O_2 reacts with H_2 after CO light-off, which results in a reduction of CO_2 selectivity by about 40%. A new route for CO_2 formation through the indirect CO oxidation with the OH(S) intermediate species is proposed and explains the observed enhancement of H_2 addition on CO conversion temperature dependency.

2.7. Kinetic studies—experiments on mono- and bifunctional reaction paths

In a mechanistic study, Pt-, Ru-, Rh/γ-Al_2O_3 catalysts were investigated for their elementary reaction steps [36]. Following literature, it was aimed to engage either of two monofunctional reaction paths, i.e. competitive adsorption of CO and O_2 on noble metal surface followed by a Langmuir–Hinshelwood step or CO adsorption on an O_2-covered site with subsequent CO_2 desorption. To promote even further the activity of the noble metals, Ru/ceria and Rh/ceria catalysts were prepared on alumina wash-coats so as to achieve CO adsorption onto the noble metal and take advantage of the O_2 storing capabilities of ceria and thus exploit the so-called bifunctional path, where CO is adsorbed onto the noble metal and interacts with the O_2 from ceria present. The two catalysts, namely 5% Ru/5% CeO_2/γ-Al_2O_3 and 5% Rh/5% CeO_2/γ-Al_2O_3, displayed higher activity with respect to Pt/γ-Al_2O_3 yet not with respect to Ru/γ-Al_2O_3 and Rh/γ-Al_2O_3. The overall lower activity as compared to the

Table 3
Physical properties of fresh, custom-prepared PrOx catalysts [36]

Catalyst	Overall loading (wt.%)	Max. pore diameter (nm)	BET specific surface area (m^2/g)	Overall catalyst mass (mg)
Pt/γ-Al_2O_3	5	4	217	250
Rh/γ-Al_2O_3	5	6	134	250
Ru/γ-Al_2O_3	10	5	60	150
Ru/CeO_2/γ-Al_2O_3	5	20	58	250
Rh/CeO_2/γ-Al_2O_3	5	8	50	250
Pt-Ru/γ-Al_2O_3 (1Pt:1Ru)	5	4	182	250
Pt-Co/γ-Al_2O_3 (1Pt:1Co)	5	14	65	250
Pt-Rh/γ-Al_2O_3 (1Pt:1Rh)	5	9	161	250
Pt-Rh/α-Al_2O_3 (1Pt:1Rh)	5	37	11	250

equivalent noble metal on alumina catalysts was considered to be due to the catalyst preparation method. The surface area of the Rh/CeO_2/γ-Al_2O_3 catalyst (Table 3) was significantly lower than that of Rh/γ-Al_2O_3 thus affecting activity. The low reduction temperature used was considered to be insufficient to promote noble metal ceria interaction but also the presence of high amounts of O_2 may have limited the effect of ceria on overall activity [37,38].

An alternative to the bifunctional path using ceria may be achieved by creating separate active sites for CO and O_2 adsorption through the addition of metal ions, such as Ru, Co or Rh [36]. Thus, catalysts with equal loading of Pt and the second noble metal on γ-alumina were prepared and tested. Pt-Co/γ-Al_2O_3 showed high activity at temperatures up to 120 °C but the rate of conversion decreased at even higher temperatures implying that temperatures well above the ones investigated would be needed in order to accomplish complete CO oxidation. Overall, three fresh catalysts achieved 100% conversion (CO below 5 ppm which was the detection limit of the GC) at temperatures up to ca. 150 °C and GHSV of 15,500 h^{-1}. More specifically, 2.5% Pt-2.5% Ru/γ-Al_2O_3 was found to achieve complete CO conversion at a temperature of 126 °C, 5% Rh/γ-Al_2O_3 at 140 °C and 2.5% Pt-2.5% Rh/γ-Al_2O_3 at 143 °C. The operating window for Pt-Ru/γ-Al_2O_3 was up to 130 °C while for the other two catalysts it was at least up to 155 °C indicating no significant CO desorption taking place, neither the presence of the reverse water–gas shift reaction nor of the methanation reaction for all temperatures investigated. When increasing the O/CO ratio from 2 to 8, with all catalysts a maximum CO elimination from the reformate stream was achieved with an O/CO ratio of 8 as expected.

2.8. Catalyst composition—impact on activity and selectivity for precious metal and non-precious metal catalysts

2.8.1. Au/CeO_2, CuO/CeO_2 and Au/α-Fe_2O_3 catalysts

Au/CeO_2, CuO/CeO_2 and Au/α-Fe_2O_3 catalysts were tested in a stack-like micro-reactor for the PrOx reaction [39]. The CeO_2-supported catalyst was prepared by coating of micro-structured stainless steel foils with ceria nano-particles, subsequent calcination in air at 450 °C and impregnation with gold or copper solutions. This way, 3 wt.% gold, respectively, 1.9 wt.% copper were introduced into the ceria support. The Au/α-Fe_2O_3 catalyst was prepared by impregnating the stainless steel foils with an iron solution and impregnation of the iron salt crystals generated with gold solution, which was performed without an intermediate calcination step. Finally, the sample was calcined at 400 °C. The adhesion of the coatings containing iron oxide to the foils was not very strong, as documented by cracks found with electron microscopy. The thickness of the catalyst coatings was 0.3–3 μm for the Au/CeO_2/CuO/CeO_2 catalysts and 1–10 μm for the Au/α-Fe_2O_3 catalysts. The size of the gold nano-particles ranged between 50 and 200 nm. The feed for catalyst testing was composed as 46–53% N_2, 6% O_2, 1–8% CO, 40% H_2. The GHSV amounted to 257,000 h^{-1}. At a feed composition of 40% H_2O, 8% CO and 6% O_2 (balance nitrogen), which corresponds to a stoichiometric O/CO ratio of 1.5, and 150 °C reaction temperature, the highest conversion (79%) was achieved at the copper catalyst, followed by the Au/CeO_2 catalyst, which converted 60% of the carbon monoxide (see Fig. 14).

The Au/α-Fe_2O_3 catalyst showed a lower conversion of 20%. CO selectivity exceeded 50% for the copper catalyst at temperatures between 180 and 210 °C [39]. The performance of the copper catalyst was also investigated under more realistic conditions of 1% CO in the feed. More than 99% CO conversion was achieved at lower temperatures between 140 and 180 °C, whereas CO selectivity was only 20% at the very high O/C ratio of 12.

2.8.2. Rh/Al_2O_3 and Rh/K/Al_2O_3 catalysts

In another study, Rh/Al_2O_3 and Rh/K/Al_2O_3 catalysts were prepared by wash-coating the alumina, dip-coating the potassium and incipient wetness impregnation of the rhodium [40]. The catalyst was reduced in a mixture of 10% hydrogen in nitrogen prior to testing. The feed was composed of 40% H_2, 20% CO_2, 0.2–1.0% CO and 0.2–1.5% O_2 on a dry basis. Ten

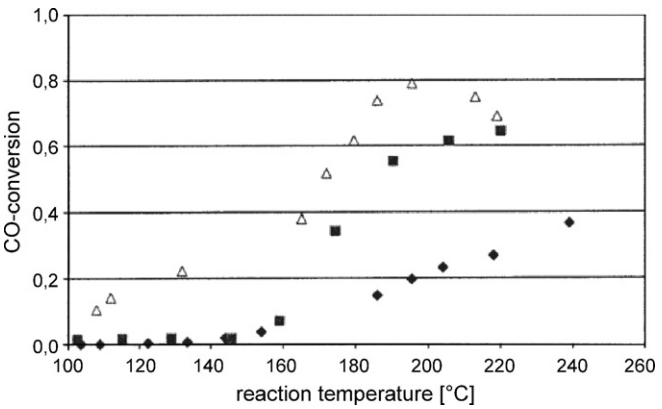

Fig. 14. Experimental results for CO conversion of the PrOx reaction vs. reaction temperature for an average residence time of 14 ms. (◆) Au/α-Fe_2O_3; (■) Au/CeO_2-II; (△) Cu/CeO_2. Eight percent CO, 40% H_2, 6% O_2, balance nitrogen [39].

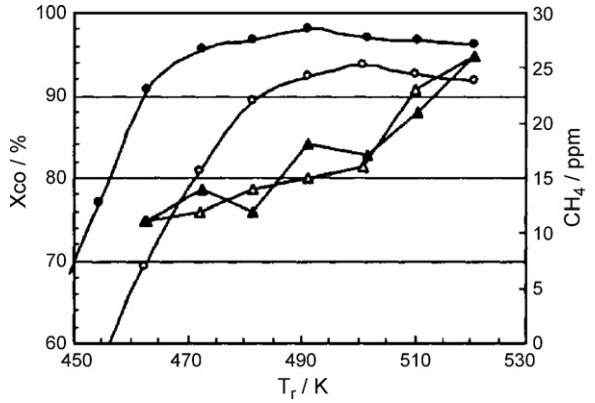

Fig. 15. CO conversion vs. reaction temperature in a micro-channel reactor. CO = 5000 ppm; GHSV = 500 000 h^{-1}; O_2/CO ratio = 1.0 (○, △), 1.25 (●, ▲). (○, ●) CO conversion; (△, ▲) outlet CH_4 concentration [40]. Rh/K/Al_2O_3 catalyst (exact composition not provided).

percent water was added to the feed and the GHSV amounted to 20,000 h^{-1}. The Rh/K/Al_2O_3 catalyst outperformed its potassium free counterpart when tested in ceramic monoliths.

CO oxidation was performed in a stack-like micro-reactor for catalyst testing in which four micro-structured foils made of stainless steel formed the stack. The foils were 340 μm thick, carrying 48 channels of 170-μm depth and 500-μm width [40].

At 300 °C, 1200 ppm methane was found at standard conditions [40]. Tests in the micro-structured reactor at the very high GHSV of 500,000 h^{-1}, 230 °C and O_2/CO ratio of 1.0, revealed a very low CO concentration of less than 20 ppm at the reactor outlet regardless of the feed concentration. Less than 30 ppm methane was detected under these conditions. Increasing the O_2/CO ratio above 1.0 did not further improve this performance (see Fig. 15).

A CO conversion of 93.6% was found for the Rh/Al_2O_3 compared with more than 99% at 200 °C and O_2/CO ratio of 1.0 or higher [40]. The highest conversion achieved was 99.82% for a CO concentration of 5000 ppm, which corresponds to less than 10 ppm at the reactor outlet. At reaction temperatures exceeding 250 °C, significant amounts of methane were formed owing to the methanation reaction, showing a selectivity of rhodium towards methanation under the conditions of the water–gas shift reaction.

2.8.3. Alumina based wash-coat catalysts

Another catalyst preparation study focused on the industrially important wash-coating technique, both directed to custom-prepared and commercially available powder wash-coat catalysts. In the case of custom catalysts, stainless steel plates were coated by first applying manually a γ-alumina or an α-alumina wash-coat onto the entire length of the etched stainless steel channels [36]. An alumina suspension was prepared from γ-alumina or α-alumina, deionised H_2O, polyvinyl alcohol binder and acetic acid. The wash-coated plates were then calcined for 2 h at 600 °C. Incipient wetness impregnation was then performed with aqueous solutions of H_2PtCl_6, $Co(NO_3)_2$, $RhCl_3$ or mixtures thereof (Table 3).

In the case of commercially available powder catalysts, the procedure for applying commercial powder catalysts (Degussa) as wash-coats was similar to that described above, but the impregnation step was omitted [36]. For bimetallic catalysts, either a commercial Pt/γ-alumina catalyst was mixed together with a commercial Rh/γ-alumina catalyst to form one wash-coat or a commercial catalyst, such as Rh/γ-alumina was mixed together with ceria. After a second calcination step (performed at 600 °C unless otherwise indicated), the catalysts were (unless otherwise indicated) mildly reduced under a flow of 55% H_2 in N_2 at 500 ml/min (STP) while initially being heated at a ramp rate of 3 °C/min from room temperature to 130 °C and then kept over for 1 h at 130 °C. The reactor was then purged with N_2 while cooling down. The catalyst properties are listed in Table 3. The surface area and maximum pore diameter of the fresh catalysts were determined through N_2 adsorption.

Using the catalysts described in Section 3.1.2 and detailed in Table 3, a stainless steel stacked reactor was operated in an integral mode to test catalyst performance, particularly to examine the effects of temperature, O/CO ratio and H_2O on catalyst activity [36]. Tests were carried out with catalyst loadings as shown in Table 3, under atmospheric pressure and a total flow rate of 550 ml/min (STP), which corresponds to a WHSV of 130 $dm^3/(h\ g_{cat})$ in most cases (if the catalyst mass amounted to 250 mg). A special gas mixture consisting only of H_2, CO_2 and CO was applied simulating the dry reformate. It was composed of 57% H_2, 21% CO_2, 1.1% CO, 4.5% O_2, balance N_2. The ratio of N_2 to O_2 at the feed was approximately that of air as in a real fuel processor. The wet feed was composed of 54% H_2, 19% CO_2, 0.9% CO, 3.8% O_2, 10% H_2O, balance N_2. The ratio of N_2 to O_2 was in this case slightly below that of air. For all experiments performed the product consisted only of H_2, CO_2, CO, H_2O, O_2 and N_2.

The CO conversion of the nine fresh catalysts in a dry feed (with excess H_2 and CO_2) is shown in Fig. 16 [36].

5% Pt/γ-Al_2O_3 was chosen as reference catalyst and showed a conversion of up 14% at 155 °C [36]. This was the least active catalyst as other noble metal catalysts, such as 10% Ru/γ-Al_2O_3

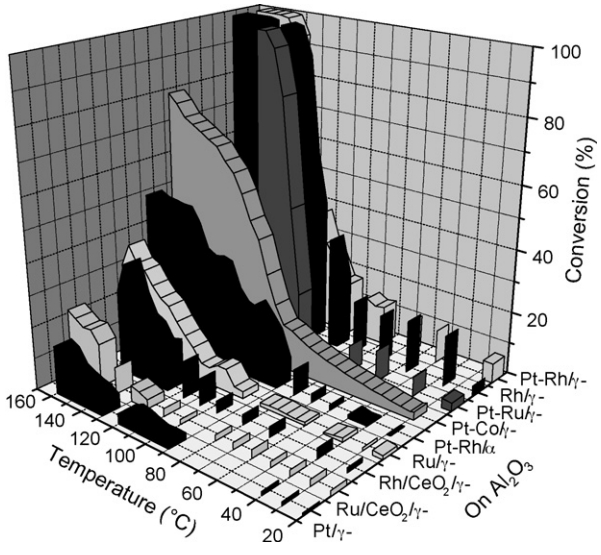

Fig. 16. CO conversion over various catalysts with respect to temperature at a GHSV of 15,500 h^{-1} [36].

and 5% Rh/γ-Al_2O_3, showed conversion levels of 30% and 100%, respectively, at 155 °C.

Even though Pt-Ru/γ-Al_2O_3 was the most active fresh catalyst, it also proved to be the least stable (full conversion only for less than 20 min) [36]. The next most active catalyst, Rh/γ-Al_2O_3, exhibited a much better stability. It remained stable for up to 20 h at which point the deactivation became evident as CO levels exceeded 10 ppm and retained an increasing trend for another hour. It was the Pt-Rh/γ-Al_2O_3 catalyst, which after 21.5 h exhibited no evident deactivation. To achieve 100% CO conversion over this catalyst, a temperature of ca. 143 °C was required at which almost all of the O_2 was depleted (99.6% conversion). Thus, the most favourable catalyst using the present catalyst preparation method, catalyst pre-treatment and reaction conditions was found to be Pt-Rh/γ-Al_2O_3 as it exhibited the best stability with relatively good activity and selectivity. However, it was not possible to achieve full conversion at an O/CO ratio of 6 (which would reduce the H_2 loss). At 153 °C, the maximum conversion was 95.6% reducing CO levels down to 493 ppm. Above this temperature, conversion decreased again owing to desorption of CO.

2.8.4. ZSM-5 zeolite catalysts

Zeolite ZSM-5 catalysts were prepared by the secondary growth method in micro-reactors, which consists of a seeding step of the micro-channels followed by hydrothermal treatment at 150–170 °C, using a gel with a molar composition of H_2O:SiO_2:NaOH:TPAOH:Al_2O_3 = 987:21:3:1:0.105 [41]. After the synthesis the supports were submitted to a calcination treatment at 480 °C for 8 h in order to remove the template from the zeolite pores. Subsequently, Pt was introduced by conventional ion-exchange with an aqueous $[Pt(NH_3)_4](NO_3)_2$ solution. The final Pt content was then determined by EDX.

The ZSM-5 catalyst samples were investigated applying the same feed composition as used in Section 2.8.3 but without addition of water [41]. Full conversion could be achieved at 170 °C reaction temperature over the sample containing 4.2 wt.% Pt (see Fig. 17). Thus, zeolite-based catalysts offer another promising route for catalysing the preferential oxidation of carbon monoxide.

2.9. Active site dispersion

Calcination temperature was reduced from 600 to 400 °C in order to achieve higher noble metal dispersion [42]. A Pt-Rh/γ-Al_2O_3 calcined catalyst at 400 °C converted the CO by more than 99.9% for a test duration of more than 180 h at a low O/CO ratio of 3 (see Fig. 18; see results at 600 °C under Section 2.7.2 for comparison). Distinct from the samples described above, this catalyst was not pre-treated by any reduction procedure. Later, catalysts prepared this way were applied successfully in a small methanol fuel processor. Two preferential oxidation reactors were operated in series to allow for stable removal of the CO prior to the fuel cell.

2.10. Thoughts on process engineering and scaling-out

Some thoughts on process engineering and scale-out of micro-structured reactors were given with a focus on achieving compactness for fuel processing systems and comparing them to packed-bed reactor technology, which does not scale down in a feasible manner [33]. In this context, a silicon micro-channel reactor was wash-coated on the channel walls by a 2% Pt/Al_2O_3 catalyst. The silicon micro-reactor performed as expected. The O_2 and CO conversion both increased with temperature. O_2 conversion reached 100% at about 210 °C; CO conversion declined again beyond 210 °C. The selectivity to CO oxidation was fairly stable near 45% until about 210 °C and then declined.

From there, distinct process engineering advantages of the micro-reactor are proposed, such as flexibility of customizable reactor designs, integration of structural and functional features, low pressure drop and optionally efficient heat management [33]. These features are said to be hardly achievable by using conventional packed-bed reactors.

Based on the results obtained from the single micro-reactor system, a prototype scale-out method for the micro-reactors has been developed [33] (see Fig. 19). The micro-reactors are stacked and bonded using glass frit bonding with commercially available VITTA1 glass transfer tapes. A pre-bake is carried out at 400 °C to burn out the binder in the tape and the micro-structured parts are contacted face-to-face by applying a small pressure. Bonding

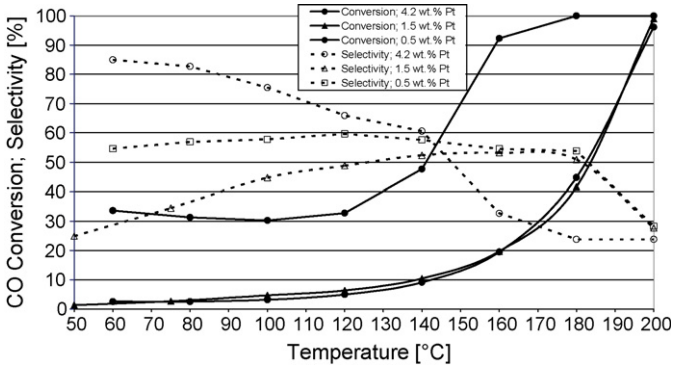

Fig. 17. CO conversion and CO selectivity as determined for different Pt-ZSM-5 catalysts vs. reaction temperature; O/CO inlet ratio of 4 and 180 N dm^3/(h g_{cat}) [41].

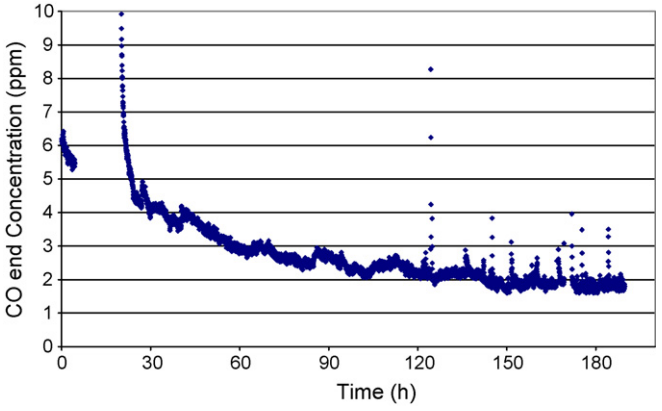

Fig. 18. CO concentration in the off-gas as determined for a Pt-Rh/γ-Al_2O_3 calcined at 400 °C at 160 °C reaction temperature, O/CO inlet ratio of 3 and 180 N dm^3/(h g_{cat}) [42].

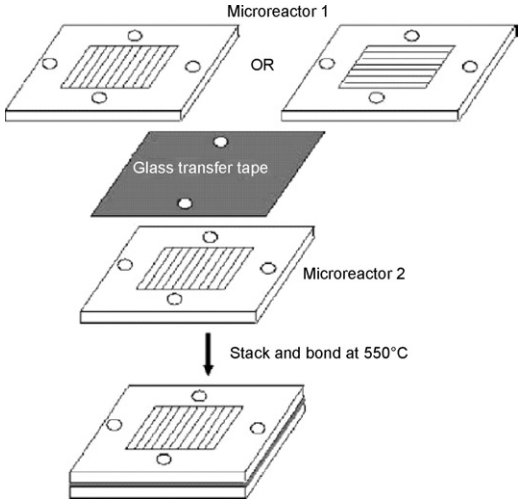

Fig. 19. Scale-up methodology for silicon micro-reactors using glass frit bonding [33].

is done by a temperature ramp up to 550 °C. Proof of principle was achieved for a double-layer stack of micro-reactors and tests for bond strength and leak tightness were done with success.

2.11. System integration—integrated micro-structured PrOx heat-exchanger-reactor for 100 W fuel processor

An integrated preferential oxidation-heat exchanger system (PrOx-Heatex) was optimised in performance by system integration. This PrOx-Heatex device needs to recover at least 80% of the available heat to ensure a high fuel processor efficiency [43]. The available heat consists of 11 W generated by the preferential oxidation reaction and 13 W released by cooling down the hot reformate gas from 250 to 60 °C, the operating temperature of the fuel cell. The recovered heat is used to preheat the combined fuel cell anode and cathode exhaust gas, which still contains 5% of hydrogen, before it is sent to the catalytic burner [44]. A selective Pt-Ru/α-Al_2O_3 catalyst is used to promote the oxidation of carbon monoxide over the oxidation of hydrogen.

The PrOx-Heatex integrated micro-reactor consists of three counter-current heat exchangers (see Fig. 20 top) [44]. A first-hour prototype was developed with reversibly sealing the three heat exchanging sections for thermal separation from each other and from the top and bottom housing parts by 4-mm thick Klingersil® plates (see Fig. 20 bottom left). Actually, many of the catalysts performance data discussed in the scope of this paper were generated in this reactor.

Subsequently, a much more compact second-generation device was made (see Fig. 20 bottom right). In the first (high-temperature) heat exchanger, the hot reformate gas is cooled down to the reactor temperature [44]. The second heat exchanger is the actual preferential oxidation reactor. It contains 1.5 g of catalyst applied on the walls of the reaction channels using a wash-coating technique with a thickness of 50 μm. The reactor has been designed to establish a decreasing temperature profile in the reaction zone from 170 to 130 °C.

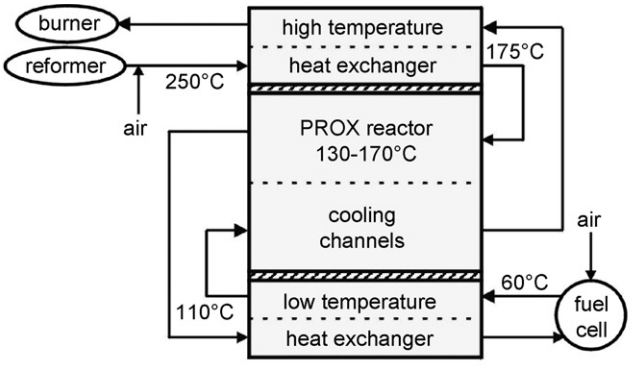

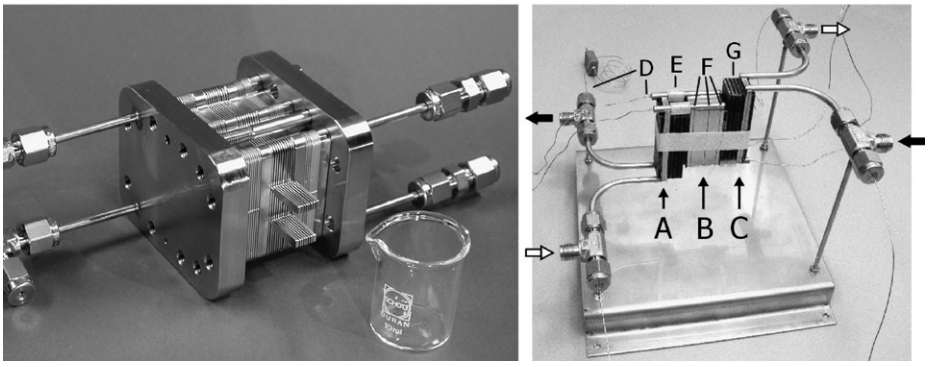

Fig. 20. (Top) Schematic drawing of the integrated preferential CO oxidation-heat exchanger (PrOx-Heatex) micro-device. The temperatures of the reformate and coolant gas streams are indicated. (Bottom left) First PrOx-Heatex prototype. (Bottom right) Assembled second-generation PrOx-Heatex micro-device consisting of a low temperature heat exchanger (A), a preferential CO oxidation reactor (B) and a high temperature heat exchanger (C); (D) thermocouples, (E) tube connection, (F) thermocouple channels and (G) insulating material [44].

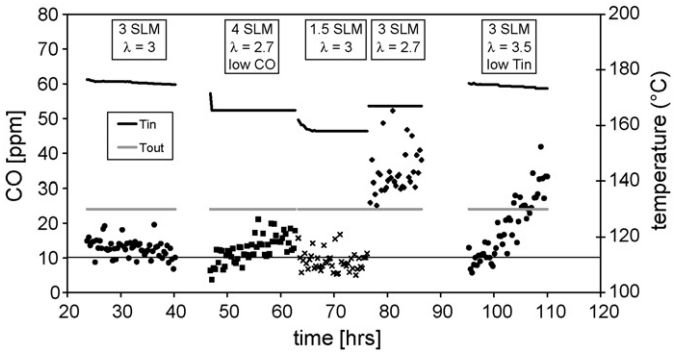

Fig. 21. Reactor temperature and CO outlet concentration as a function of time for various flow rates (SLM, standard liters per minute) and oxygen excess values (λ = 2 times inlet molar flow rate of oxygen over the inlet molar flow rate of carbon monoxide). The CO inlet concentration is 5000 ppm and in the 'low CO' experiment the CO inlet concentration is 3750 ppm. The 'low T_{in}' experiment was done at a lower inlet temperature of the reformate and coolant gas to the device (200 and 30 °C instead of 240 and 60 °C, respectively) [44].

In this way, a high activity at the beginning of the reaction zone is combined with a high selectivity at the end of the reaction zone. In the third (low temperature) heat exchanger, the CO-free reformate gas is cooled down further to a temperature of 60 °C to extract its remaining thermal energy.

The design process was started by optimizing the geometry of the flow distribution chambers to ensure equal flow rates in the individual micro-channels using 3D fluid dynamics simulations [44]. In the second step, a 2D heat transfer model was used to verify that all micro-channels would also experience equal temperature profiles. When several components operating at different temperatures are integrated into a small device, transfer of heat between the components is hard to avoid. Therefore, it is not sufficient to design the individual components (e.g. distribution chambers, reactor, heat exchangers) separately. In a third step, an integral model was used, consisting of rapidly converging 1D sub-models of the separate units. The heat exchangers and the reactor were constructed from 500 μm thick stainless steel plates, in both sides of which micro-channels and flow distribution chambers were etched (more information about the PrOx-Heatex system design, layout and construction can be found in refs. [44,45]).

The PrOx-Heatex device was tested in a set-up capable of feeding a reformate gas with a variable flow rate and composition and a separate flow of nitrogen to serve as the coolant gas [44]. The reformate gas stream was first preheated to 350 °C. Due to external heat losses, reformate entered the PrOx-Heatex device at a temperature between 180 and 260 °C, depending on the flow rate. The temperature at the reformate outlet of the reactor part was controlled by varying the coolant flow. Pure nitrogen was used as coolant gas, which was preheated to 60 °C before entering the device. The standard reformate gas consisted of 0.5% CO, 0.88% O_2, 56% H_2, 18% CO_2, 10% H_2O, 0.75% N_2 and balance helium. The standard flow rate was 3 SLM (standard liters per minute), corresponding to the amount of hydrogen needed for a 100 W_e fuel cell. Oxidation experiments were performed at varying oxygen excess and varying reactor outlet temperature. The reformate gas was analyzed for oxygen and CO at the inlet and outlet of the PrOx-Heatex device to determine conversion and selectivity.

During the test program the PrOx-Heatex device was operated continuously for five days. During this period, several shorter experiments (<2 h) were performed to scan a wide range of operating conditions as well as several longer experiments (>10 h) to study the stability of the catalyst [44] (see Fig. 21). In the experiments, the reactor outlet temperature was kept constant by regulating the coolant flow rate to the device. Consequently, the reactor inlet temperature changed depending on the operating conditions. For several combinations of flow rate and oxygen excess, the micro-structured device is capable of reducing the CO concentration in a realistic reformate gas from 5000 to about 10 ppm at a flow rate of 7.4 $mmol_{CO}\ s^{-1}\ kg_{cat}{}^{-1}$. However, the CO conversion is not always stable. Especially in the last experiment, catalyst deactivation became evident as the CO concentration remained close to 10 ppm in the first 5 h, but then rose to about 30 ppm during the next 10 h. The catalyst activity compares well with the results of Dudfield et al. [27], who reduced the CO concentration in a reformate stream from 7000 to below 10 ppm in a dual-stage heat exchanger-reactor using a similar Pt-Ru/Al_2O_3 catalyst, up to a flow rate of 5.7 $mmol_{CO}\ s^{-1}\ kg_{cat}{}^{-1}$.

2.12. System integration—integrated micro-structure PrOx heat-exchanger-reactor for a 20 kW fuel processor

A combined methanol steam reformer and combustor with a consecutive CO clean up by preferential oxidation was developed in the Mercatox program [25]. Firstly, different catalysts shaped as micro-spheres were tested for their performance in the PrOx reaction in a test reactor, which was similar to a macroscopic shell-and-tube heat-exchanger (see Fig. 22).

The catalysts tested are shown in Table 4. A 10 Ndm^3/min feed composed of 75.0% H_2, 0.7% CO, balance CO_2 and air for oxidation was fed into the test reactor carrying 230 cm^3 catalyst micro-spheres of 1-mm diameter [25]. Of the non-precious metal catalysts, the sample merely composed of hopcalite showed the highest activity achieving almost full conversion in the temperature window between 130 and 160 °C. The minimum CO output achieved amounted to 40 ppm. A

Table 4
Catalysts evaluated for CO-PrOx application [25]

Catalyst carrier	Catalyst code	Active component 1 (wt.%)	Active component 2 (wt.%)
Hopcalite	LU-1	–	–
Aluminium stannate	LU-3	Cu 5	La 3
Ferric oxide	LU-3	Cu 3	Ce 2
Silica + 4 wt.% Ce	LU-4	Mn 8	Cu 2
Silica	LU-5	Pd 2.5	–
Silica	LU-6	Ru 2	–
Silica	LU-7	Ru/Pt 2.25	–
Alumina	LU-8	Ru/Pt 3.5	–
Hopcalite	LU-9	Ru/Pt 2.5	–

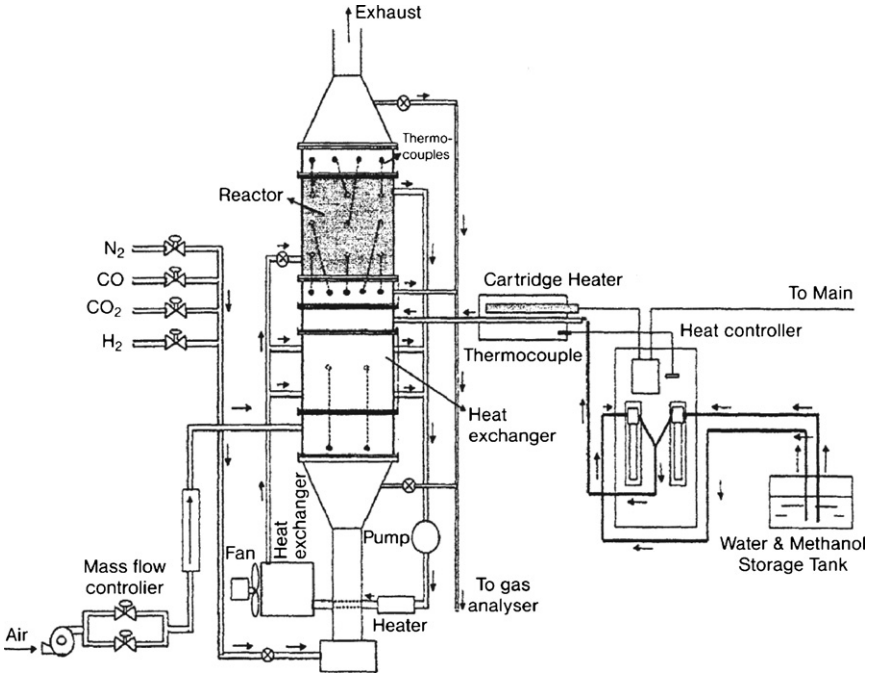

Fig. 22. Schematic of the catalyst test assembly [25].

minimum O_2/CO ratio of 2.5 was determined for this catalyst to achieve carbon monoxide conversion exceeding 90%. At a O_2/CO ratio of 2.0, this catalyst converted 98% of the carbon monoxide and as much as 4.6% of the hydrogen, which corresponds to 3.5% absolute loss of hydrogen. Of the precious-metal catalysts, the Pt/Ru samples showed the highest activity, corresponding to conversions exceeding 99.8%. Notably, the sample based on the hopcalite carrier produced this high level of conversion in the wide temperature window of 90–160 °C and achieved low CO output of 7 ppm (see Fig. 23).

2.13. Process-flow integration—pilot (2 kW_e) prototype PrOx reactor, operated with WGS off gas

Process-flow integration was demonstrated for a pilot (2 kW_e) prototype PrOx reactor, operated with WGS off gas as a practical example for reactor development for use in fuel processors [46,47]. This work involved meeting the specifications of an actual device, such as catalyst load, size and weight, thus approaching prototype design. The target was to reduce a 1% CO process flow coming from the WGS reaction (2 kW_e stream) to less than 10 ppm for use in a PEM fuel cell, and to reduce size and weight, since the application was transportation.

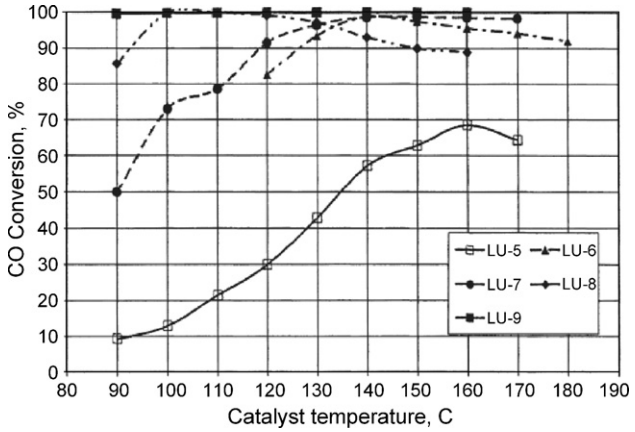

Fig. 23. Experimental results for the conversion of CO on precious metal catalysts [25]. See Table 4 for the catalyst codes LU-5 to LU-9. Feed: 0.7 vol.% CO, 75 vol.% H_2, bal. CO_2; 10 SLPM flow rate; 230 cm^3 microsphere catalyst volume; O/CO ratio not provided.

The reactor comprised a multi-chamber design, with each chamber filled with catalyst, and thin fluidic cooling panels sandwiched in between [46,47]. The catalyst was coated on high thermal conductivity porous material, following the engineered catalyst approach, encompassing, e.g. felts or foams. The latter was actually applied in this case. This allows fast heat transfer both by convection through the gas phase and conduction from the foam to the cooling panel and should avoid any hot spots. As another means of maintaining constant temperature, air was added stage-wise, rather than being fed all-at-once at the reactor entrance to have better control over reaction speed. One big advantage of said reactor design is to carry high catalyst loads, up to nearly 70% of the volume (excluding housing walls and headers). There is also flexibility in the load of catalyst per chamber and, by varying the catalyst volume, the heat transfer efficiency can be modulated to compensate for the decreasing reactivity of the PrOx reaction along the reaction path.

As first stage catalyst (CO concentration 1%) a non-precious metal catalyst from SudChemie was used [46,47]; as second-stage catalyst (CO 330 ppm) two precious metal catalysts from Engelhard were tested and finally the high-temperature catalyst (200 °C; close to the first-stage temperature) was chosen among these two. For both stages, <97% conversion was achieved. The PrOX reactor was composed of four chambers and the SudChemie catalyst was loaded into the first three followed by the Engelhard catalyst in the last chamber.

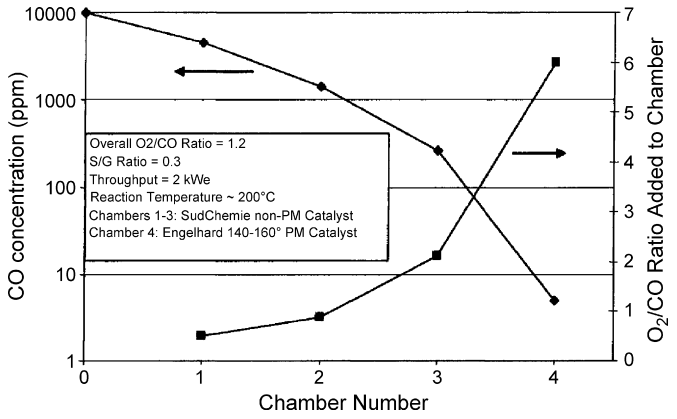

Fig. 24. CO concentration reduction by a reactor with two-staged arrangement of a non-precious metal catalyst from SudChemie (loaded in first three reaction chambers) and a precious metal catalyst from Engelhard (loaded in fourth and last chamber) [46].

The CO content was reduced from 1% to less than 10 ppm with an overall O_2:CO ratio of 1.2:1 (see Fig. 24). The O_2:CO addition, however, was done stage-wise, starting with a ratio of 0.5:1 and increasing it along the flow path, finally to 6:1 in the last chamber. Temperature profile measurements in the catalyst bed showed a periodic profile with temperature spreads within ±20 °C throughout the reactor. The adiabatic temperature rise can exceed 100 °C, which illustrates the good temperature control achieved by the staged heat exchangers and air addition.

2.14. Process-flow integration—use of real-case wet feeds

In order to investigate the effect of H_2O on the activity and selectivity of the Pt-Rh/γ-Al_2O_3 catalyst, a wet feed was passed through the reactor [36]. H_2O had a dramatic effect on CO conversion between 125 and 140 °C (see Fig. 25). The slight drop in CO conversion of about 0.1% experienced between 130 and 145 °C during the experiment with the wet feed is attributed to the fact that selectivity dropped due to partial CO desorption thus allowing more H_2 to be converted. The water–gas shift reaction is not believed to have been significant as there was O_2 consumption taking place parallel to CO conversion while there was no H_2 production observed. Fig. 25 also confirms the small influence H_2O has on selectivity.

In the presence of H_2O, selectivity was decreased by a maximum of 1.5% at a temperature of 130 °C while the effect became insignificant at 140 °C [36]. This small influence indicates the increase of both the rates of CO oxidation and H_2 oxidation in the presence of H_2O (and in effect of OH groups). The operating window of the catalyst was therefore found to be increased in the presence of H_2O. Similar observations have been made by Manasilp and Gulari [39] who investigated CO oxidation over a Pt/Al_2O_3 catalyst and by Yan et al. [26] who investigated CO oxidation over a Pt-Co/Al_2O_3 catalyst. Manasilp and Gulari [48] proposed the possibility that the OH groups formed on the catalyst upon H_2O adsorption are better oxidants than O_2 itself.

2.15. Heat recovery efficiency and exergy analysis

The heat recovery efficiency of an integrated preferential oxidation-heat exchanger device (PrOx-Heatex) (see Section 2.11) was determined experimentally from the outlet temperature of the coolant gas [44]. This heat recovery efficiency was calculated as a function of the reformate gas flow rate (see Fig. 26). The overall heat recovery of the device varies between 73% and 95%, with the higher numbers corresponding to higher flow rates and higher oxygen excess. The target heat recovery of 80% for the PrOx-Heatex unit is thus amply met for most operating conditions, which indicates that there is room to reduce the insulation thickness. The results suggest that the insulation thickness can be decreased to 2 cm, which will decrease the total volume of the device including the insulation to 0.6 l.

As shown by exergy analysis and volume and weight benchmarking, the efficiency of integrated PrOx-Heatex systems may compete with the current energy carriers as rechargeable batteries or combustion engines (see Fig. 27) [49].

2.16. PrOx-Heatex: comparing conventional fixed-bed and micro-reactor technology

A comparison was made between preferential oxidation-heat exchanger (PrOx-Heatex) reactors based on fixed-bed technol-

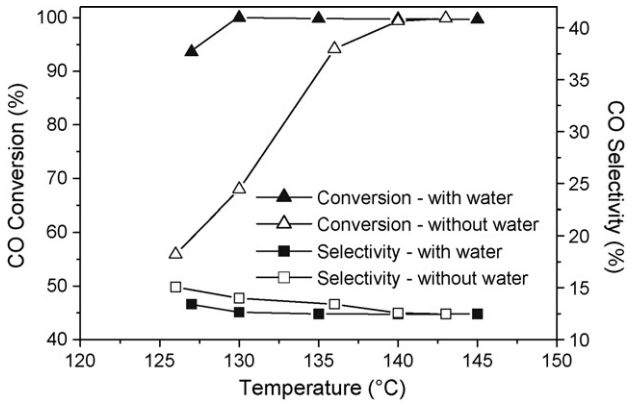

Fig. 25. CO conversion and selectivity over Pt-Rh/γ-Al_2O_3 of feeds with and without H_2O, at varying temperatures, O/CO inlet ratio of 8 and GHSV of 15,500 h^{-1} [36].

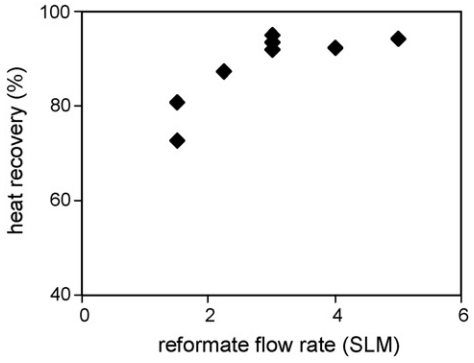

Fig. 26. Heat recovery efficiency of the PrOx-Heatex device as a function of the reformate gas flow rate; the oxygen excess λ varies between 2.5 and 6 (SLM, standard liters per minute) [44].

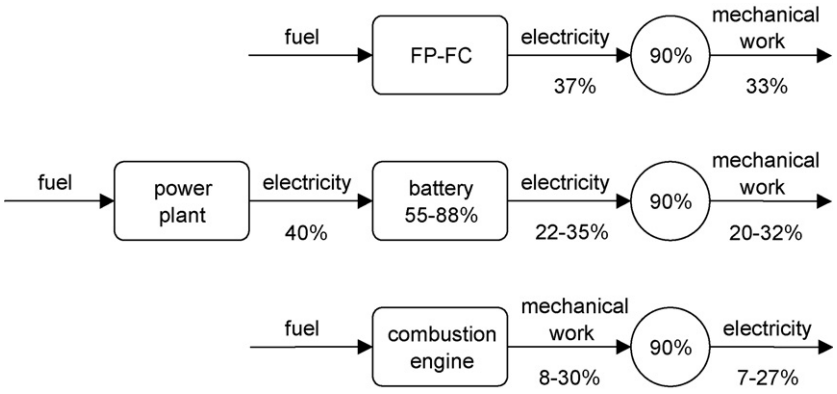

Fig. 27. Comparison of exergetic efficiency between the FP and FC system, rechargeable batteries and combustion engines [49].

ogy and on micro-reactor technology for system designs for 100 W_e and 5 kW_e power output [50]. The 100 W_e case is at the scale typical for portable electronics applications, while the 5 kW_e case is typical of auxiliary power units, which are used for automotive and domestic power applications. Two PrOx-Heatex designs and two reformer-burner (RefBurn) designs (see Fig. 5 and ref. [50]) are evaluated on four comparison criteria: system volume, insulation volume, system weight and required catalyst mass. Fixed design critera are used for reactor conversion, maximum reactor temperature, pressure drop and heat loss. In this way, differences in heat and mass transfer characteristics will show up as differences in the required catalyst mass and ultimately in the system's size and weight. A detailed description of this comparative study can be found in refs. [44,45].

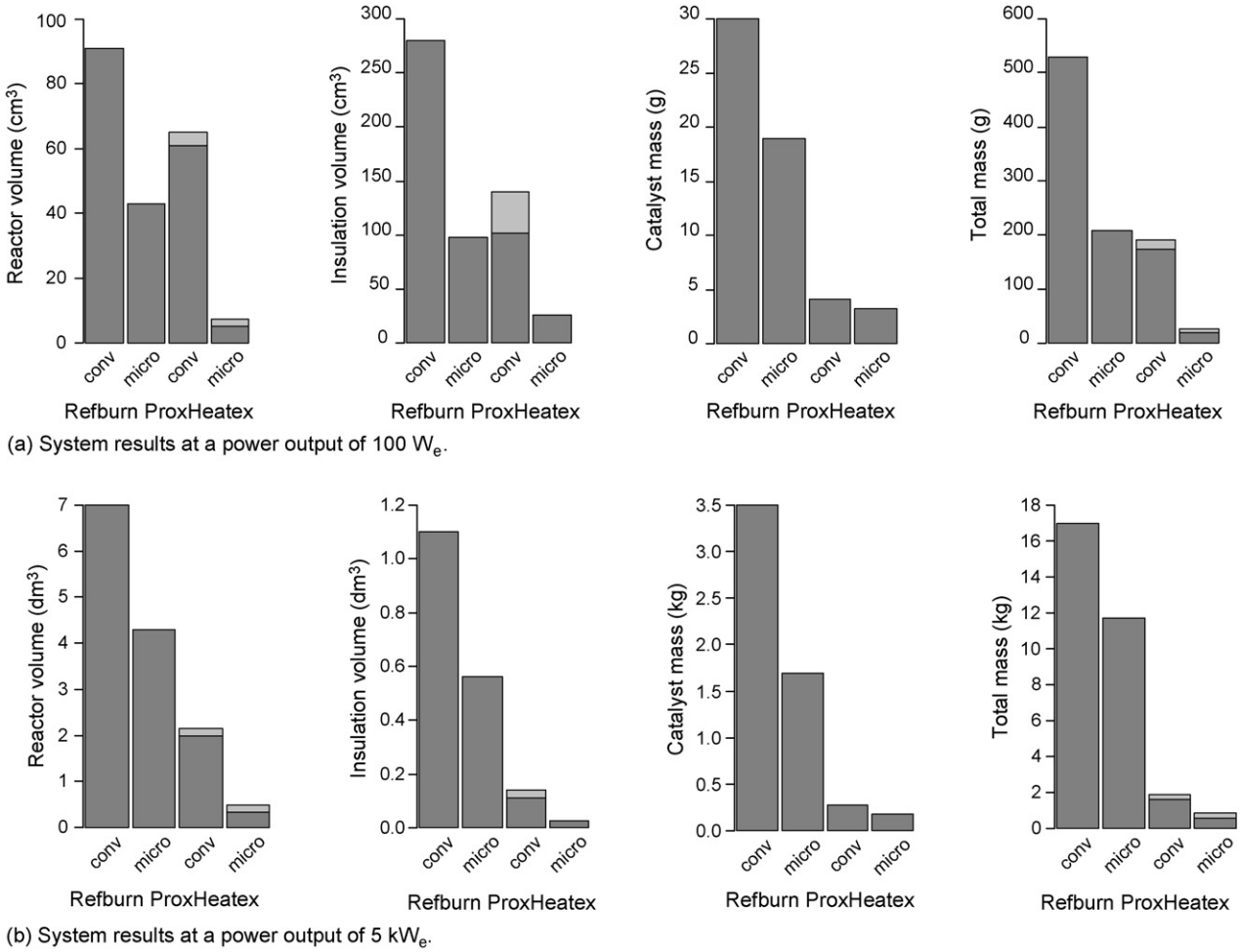

Fig. 28. Results for the quantified comparison criteria for a power output of (a) 100 W_e and (b) 5 kW_e, for the conventional fixed-bed (conv) and micro-reactor (micro) designs. Light gray parts in the PrOx-Heatex graphs indicate the fraction related to the two heat exchangers. Also shown are the results for the quantified comparison critera in case of the integrated reformer-burner (RefBurn) reactor (see Fig. 21 and ref. [50]).

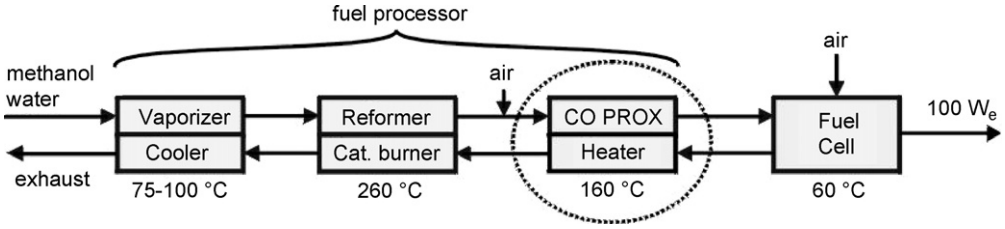

Fig. 29. The MiRTH-e fuel processor-fuel cell system [52], consisting of three integrated micro-devices and a miniature fuel cell, all working at specific temperatures. The encircled unit is the integrated preferential CO oxidation-heat exchanger (PrOx-Heatex) micro-device.

The conventional fixed-bed PrOx-Heatex devices at both power outputs consist of three separate units: a fixed-bed reactor and two compact plate-fin heat exchangers, which are the first choice for gas-to-gas heat exchange [50]. The fixed-bed reactors are designed using a two-dimensional pseudo-homogeneous model including heat transfer resistances in the catalyst bed and at the tube walls and including mass transfer resistances in the catalyst pellets. The PrOx-Heatex micro-reactors at both power outputs are considered as being constructed as a stack of micro-structured metal plates. The micro-reactors are designed using dedicated micro-reactor models including heat conduction in the micro-structured plates and mass transfer limitations in the coated catalyst layer on the micro-channel walls.

On both power output scales, the micro-reactor designs outperform the conventional fixed-bed designs, leading to significantly lower reactor volumes and weights (in case of the PrOx-Heatex device as well as in case of the integrated reformer-burner (RefBurn) micro-reactor (see Fig. 28) [50]). The scaling factors of reactor volume and reactor weight are larger for the micro-reactor systems than for the conventional fixed-bed systems, indicating that at larger scales the fixed-bed reactors will ultimately outperform the micro-reactor designs.

2.17. Methanol fuel processor process flow

Bringing CO levels to below 50 ppm does not only require an active catalyst but also good reactor design. A key issue for efficient reactor operation in terms of reducing CO to levels acceptable for PEM fuel cells is that of thermal management. Thus, a compact device is preferable in order to achieve a high surface area-to-volume ratio and high heat and mass transfer efficiencies [2b,51]. Micro-channels are known to achieve these properties in addition to lower pressure drops as compared to packed catalyst beds. Most importantly, they are suitable for wash-coating and thus improved catalyst utilisation can be achieved through the enhanced mass and heat transfer rates offered.

A typical fuel processing system for a PEM fuel cell consists of a number of units namely, a fuel tank, a start-up burner, an evaporator (if the fuel is a liquid), a reformer, a water–gas shift reactor, a selective oxidation reactor and a catalytic burner [2b]. If the fuel reformed is methanol then a water–gas shift reactor is not required as CO levels in the reformer exit stream do not significantly exceed 1%. Thus, the CO clean-up is carried out in a selective oxidation reactor alone in order to bring levels down to well below 50 ppm to ensure efficient operation of a PEM fuel cell.

To balance the heat produced and the heat required by the various units incorporated in a methanol steam reforming system, devices may be coupled (see Fig. 29).

Thus, the water methanol mixture entering the evaporator may be heated by a coupled heater (to 75–100 °C), while the hot reformate stream leaving the coupled reformer-burner device (at ca. 270 °C) may be cooled to CO oxidation temperatures (ca. 140–160 °C) by the cooler stream leaving the PEM fuel cell (at ca. 60 °C) consisting of the unutilised H_2 [52] This may be burnt catalytically to provide energy to a coupled steam reformer. The hot exit stream of the burner may then further provide energy to the methanol evaporator. Thus, a selective CO oxidation micro-structured reactor prototype was designed to function as a counter-current heat exchanger.

Within the European Union funded project MiRTH-e [52], a miniaturized fuel-processing system has been developed to generate hydrogen in situ from a methanol–water mixture, to fuel a 100 W_e fuel cell. The volume of the fuel processor was targeted to be less than 500 cm^3 with a system energy density of more than 3 MJ/kg (or more than 800 Wh/kg). This means that the combination of the fuel processor and the fuel cell should provide a 5–10-fold improvement of the energy density as compared to battery packs and hydrogen storage in metal hydrides.

Based on a dedicated second-law exergy analysis and pinch analysis of the system [49], the fuel processor is subdivided into three integrated micro-devices: a vaporizer–cooler, a reformer-burner and a preferential oxidation-heat exchanger unit. The largest exergy losses occur in the fuel cell, the burner, the vaporizer and the reformer. The overall exergetic efficiency of the system is about 37%. The total exergy loss depends predominantly on the methanol concentration in the feed and the fuel cell performance; the temperatures in the reformer and in the fuel cell have a much smaller effect.

3. Summary and outlook

A number of selective oxidation reactions carried out in micro-channel reactors have been reported in the literature. Initial reactions were often either model reactions or headed for step change by ‘dream reactions’ (typically direct routes to a valuable intermediate) with initially poor selectivity or were restricted to process development. A number of advantages of micro-flow processing were shown thereby, stemming from the

improved flow and heat- and mass-transfer characteristics of micro-reactors. In addition, suitable catalyst formulation techniques, tailored for micro-channels, were developed. Meanwhile, such advanced technology base is used mainly for the preferential oxidation (PrOx) as a gas purification step in the framework of fuel processing. Advanced catalysts involving combinations of noble metals, zeolites and other oxide supports permit CO reduction down to the ppm-level. Such catalyst-loaded micro-reactors were developed and tested. For efficient heat recovery, such reactors were integrated into devices with micro heat exchangers as well. A number of issues on the catalyst and reactor engineering level have been solved, like selectivity and efficient heat transfer. The process engineering, especially the integration into complete fuel processor plants, has just been started. At least, reports of operation under real-case process flows and at large-throughput and correspondingly large equivalent energy level (in the range of some kW) are available in open literature; the most advanced results like the fuel processor performance itself so far has been largely disclosed.

The preferential oxidation is just one step among others in the field of fuel processing. For the other reactions needed, integrated devices have been built (e.g. RefBurn/WGS-Heatex) as well up to the construction and testing of complete fuel processors. Fuel processors with micro-structured reactors are being developed up to the 10-kW range, using methanol, ethanol, bio-ethanol, iso-octane (gasoline), diesel, butane, propane and methane as fuels.

Acknowledgements

The authors gratefully acknowledge funding of part of the work presented here from the European Commission for the project 'Micro Reactor Technology for Hydrogen and Electricity' (MiRTH-e), contract number ENK6-CT-2000-00110, under the 'Energy, Environment and Sustainable Development' Programme.

The core part of this review has already been given in the conference pre-prints of the DGMK/SCI-Conference ''Oxidation and Functionalization: Classical and Alternative Routes and Sources'', October 12–14, 2005 held in Milan, Italy. Copyright to use these contents was kindly given by the DGMK editorial office, which is acknowledged hereby.

References

[1] V. Hessel, G. Kolb, J.C. Schouten, V. Cominos, C. Hofmann, H. Löwe, G. Nikolaidis, R. Zapf, A. Ziogas, E.R. Delsman, M.H.J.M. de Croon, O. de la Iglesia, R. Mallada, J. Santamaria, in: S. Ernst, E. Gallei, J.A. Lercher, Rossini, E. Santacesaria (Eds.), Conference pre-prints of the DGMK/SCI-Conference ''Oxidation and Functionalization: Classical and Alternative Routes and Sources'', Milan, Italy, October 12–14, 2005 (see also acknowledgements above).

[2] (a) V. Hessel, H. Löwe, A. Müller, G. Kolb, Chemical Micro Process Engineering—Processing and Plants, Wiley-VCH, Weinheim, 2005;
(b) V. Hessel, S. Hardt, H. Löwe, Chemical Micro Process Engineering—Fundamentals, Modelling and Reactions, Wiley-VCH, Weinheim, 2004.

[3] K. Jähnisch, V. Hessel, H. Löwe, M. Baerns, Angew. Chem. Int. Ed. 43 (4) (2004) 406.

[4] K.F. Jensen, Chem. Eng. Sci. 56 (2001) 293.

[5] A. Gavriilidis, P. Angeli, E. Cao, K.K. Yeong, Y.S.S. Wan, TransIChem 80/A (1) (2002) 3.

[6] E.V. Rebrov, M.H.J.M. de Croon, J.C. Schouten, Catal. Today 69 (2001) 183.

[7] E.V. Rebrov, M.H.J.M. de Croon, J.C. Schouten, Microreaction technology—IMRET 5, in: M. Matlosz, W. Ehrfeld, J.P. Baselt (Eds.), Proceedings of the Fifth International Conference on Microreaction Technology, Springer-Verlag, Berlin, 2001, p. 49.

[8] E.V. Rebrov, M.H.J.M. de Croon, J.C. Schouten, Chem. Eng. J. 90 (2002) 61.

[9] R. Srinivasan, I.-M. Hsing, P.E. Berger, K.F. Jensen, S.L. Firebaugh, M.A. Schmidt, M.P. Harold, J.J. Lerou, J.F. Ryley, AIChE J. 43 (11) (1997) 3059.

[10] K.F. Jensen, AIChE J. 45 (10) (1999) 2051.

[11] L.M. Hsing, R. Srinivasan, M.P. Harold, K.F. Jensen, M.A. Schmidt, Chem. Eng. Sci. 55 (2000) 3.

[12] D.J. Quiram, I.-M. Hsing, A.J. Franz, K.F. Jensen, M.A. Schmidt, Chem. Eng. Sci. 55 (2000) 3065.

[13] A. Kursawe, D. Hönicke, Microreaction technology—IMRET 5, in: M. Matlosz, W. Ehrfeld, J.P. Baselt (Eds.), Proceedings of the Fifth International Conference on Microreaction Technology, Springer-Verlag, Berlin, 2001, p. 240.

[14] H. Kestenbaum, A. Lange de Olivera, W. Schmidt, H. Schüth, W. Ehrfeld, K. Gebauer, H. Löwe, T. Richter, Stud. Surf. Sci. Catal. 130 (2000) 2741.

[15] H. Kestenbaum, A. Lange de Olivera, W. Schmidt, F. Schüth, W. Ehrfeld, K. Gebauer, H. Löwe, T. Richter, Ind. Eng. Chem. Res. 41 (4) (2000) 710.

[16] S. Kah, D. Hönicke, Microreaction technology—IMRET 5, in: M. Matlosz, W. Ehrfeld, J.P. Baselt (Eds.), Proceedings of the Fifth International Conference on Microreaction Technology, Springer-Verlag, Berlin, 2001, p. 397.

[17] O. Wörz, K.-P. Jäckel, T. Richter, A. Wolf, Chem. Eng. Technol. 24 (2) (2001) 138.

[18] E. Cao, A. Gavriilidis, W.B. Motherwell, Chem. Eng. Sci. 59 (2004) 4803.

[19] S. Walter, E. Joannet, M. Schiel, I. Boullet, R. Philipps, M.A. Liauw, Microreaction technology—IMRET 5, in: M. Matlosz, W. Ehrfeld, J.P. Baselt (Eds.), Proceedings of the Fifth International Conference on Microreaction Technology, Springer-Verlag, Berlin, 2001, p. 387.

[20] V. Hessel, W. Ehrfeld, K. Golbig, C. Hofmann, S. Jungwirth, H. Löwe, T. Richter, M. Storz, A. Wolf, O. Wörz, J. Breysse, Microreaction technology, in: W. Ehrfeld (Ed.), Third International Conference on Microreaction Technology, Proceeding of IMRET 3, Springer-Verlag, Berlin, 2000, p. 152.

[21] G. Veser, Chem. Eng. Sci. 56 (2001) 1265.

[22] K. Haas-Santo, O. Görke, K. Schubert, J. Fiedler, H. Funke, Microreaction technology—IMRET 5, in: M. Matlosz, W. Ehrfeld, J.P. Baselt (Eds.), Proceedings of the Fifth International Conference on Microreaction Technology, Springer-Verlag, Berlin, 2001, p. 313.

[23] P. Pennemann, V. Hessel, H. Löwe, Chem. Eng. Sci. 59 (22–23) (2004) 4789.

[24] A.F. Ghenciu, Curr. Opin. Sol. St. Mater. Sci. 6 (2002) 389.

[25] C.D. Dudfield, R. Chen, P.L. Adcock, Int. J. Hydrogen Energy 26 (2001) 763.

[26] J. Yan, J. Ma, P. Cao, P. Li, Catal. Lett. 93 (2004) 55.

[27] P.V. Snytnikov, V.A. Sobyanin, V.D. Belyaev, P.G. Tsyrulnikov, N.B. Shitova, D.A. Shlyapin, Appl. Catal. A 239 (2003) 149.

[28] G. Chen, Q. Yuan, H. Li, S. Li, Chem. Eng. J. 101 (1–3) (2004) 101.

[29] K. Shah, X. Ouyang, R.S. Besser, Chem. Eng. Technol. 28 (3) (2005) 303.

[30] F. Gracia, W. Li, E.E. Wolf, Catal. Lett. 91 (3–4) (2003) 235.

[31] http://www.in-situresearch.com/Prods/combi.html.

[32] X. Ouyang, R.S. Besser, J. Power Sources 141 (1) (2005) 39.

[33] S. Srinivasa, A. Dhingrab, H. Imb, E. Gularia, Appl. Catal. A: Gen. 274 (2004) 285.

[34] X. Ouyang, L. Bednarova, R.S. Besser, P. Ho, AIChE J. 51 (6) (2005) 1758.

[35] R.S. Besser, X. Ouyang, H. Chen, W.C. Shin, W. Lee, S. Pau, C.S. Pai, J.A. Taylor, W.M. S Mansfield, in: Proceedings of the AIChE Spring Meeting, vol. 171a, 26–29 April, 2004 (published on CD).

[36] C. Cominos, V. Hessel, C. Hofmann, G. Kolb, R. Zapf, A. Ziogas, E.R. Delsman, J.C. Schouten, Catal. Today 110 (1–2) (2005) 140.
[37] S. Özkara, A.E. Aksoylu, Appl. Catal. A 251 (2003) 75.
[38] I.H. Son, A.M. Lane, Catal. Lett. 76 (2001) 151.
[39] O. Görke, P. Pfeifer, K. Schubert, Appl. Catal. A 263 (2004) 11.
[40] G. Chen, Q. Yuan, H. Li, S. Li, Chem. Eng. J. 101 (1–3) (2004) 101.
[41] University Zaragoza, unpublished results.
[42] Institut für Mikrotechnik Mainz GmbH, unpublished results.
[43] P.J. de Wild, M.J.F.M. Verhaak, D.F. Bakker, International Patent WO 00/17097, 2000.
[44] E.R. Delsman, M.H.J.M. de Croon, A. Pierik, G.J. Kramer, P.D. Cobden, C. Hofmann, C. Cominos, J.C. Schouten, Chem. Eng. Sci. 59 (22–23) (2004) 4795.
[45] E.R. Delsman, Microstructured reactors for a portable hydrogen production unit, Ph.D. thesis, Eindhoven University of Technology, Eindhoven, The Netherlands, 2005 (ISBN 90-386-3036-0), http://alexandria.tue.nl/extra2/200511817.pdf.
[46] D.L. King, K.P. Brooks, C.M. Fischer, L.R. Pederson, G.C. Rawlings, V.S. Stenkamp, W.E. Tegrotenhuis, R.S. Wegeng, G. Whyatt, A. Whyatt, Fuel reformation: catalyst requirements in microchannel architectures, in: J. Wang, J.D. Holladay (Eds.), Microreactor Technology and Process Intensification, ACS Symposium Series 914, ACS Books Department, 2005 .
[47] K.P. Brooks, C.M. Fischer, D.L. King, L.R. Pederson, G.C. Rawlings, V.S. Stenkamp, W.E. Tegrotenhuis, R.S. Wegeng, G.A. Whyatt, Fuel reformation: microchannel reactor design, in: J. Wang, J.D. Holladay (Eds.), Microreactor Technology and Process Intensification, ACS Symposium Series 914, ACS Books Department, 2005.
[48] A. Manasilp, E. Gulari, Appl. Catal. B 37 (2002) 17.
[49] E.R. Delsman, C.U. Uju, M.H.J.M. de Croon, J.C. Schouten, K.J. Ptasinski, Energy Int. J., in press.
[50] E.R. Delsman, B.J.P.F. Laarhoven, M.H.J.M. de Croon, G.J. Kramer, J.C. Schouten, Chem. Eng. Res. Des. 83 (A9) (2005) 1063.
[51] G. Kolb, V. Hessel, Chem. Eng. J. 98 (1–2) (2004) 1.
[52] E.R. Delsman, E.V. Rebrov, M.H.J.M. de Croon, J.C. Schouten, G.J. Kramer, V. Cominos, T. Richter, T.T. Veenstra, A. van den Berg, P.D. Cobden, F.A. de Bruijn, C. Ferret, U. d'Ortona, L. Falk, in: M. Matlosz, W. Ehrfeld, J.P. Baselt (Eds.), Proceedings of the Fifth International Conference on Microreaction Technology, Springer-Verlag, Berlin, Germany, 2001, p. 268.